

Domain Adaptation in Agricultural Image Analysis: A Comprehensive Review from Shallow Models to Deep Learning

Xing Hu^a, Siyuan Chen^a and Dawei Zhang^a

^aSchool of Optical-Electrical and Computer Engineering, University of Shanghai for Science and Technology, No. 516, Jungong Road, Shanghai, 200093, China

ARTICLE INFO

Keywords:

Domain Adaptation, Deep Learning, Agricultural Image Analysis, Cross-Domain Transfer, Adversarial Learning

ABSTRACT

With the increasing use of computer vision in agriculture, image analysis has become crucial for tasks like crop health monitoring and pest detection. However, significant domain shifts between source and target domains—due to environmental differences, crop types, and data acquisition methods—pose challenges. These domain gaps limit the ability of models to generalize across regions, seasons, and complex agricultural environments.

This paper explores how Domain Adaptation (DA) techniques can address these challenges, focusing on their role in enhancing the cross-domain transferability of agricultural image analysis. DA has gained attention in agricultural vision tasks due to its potential to mitigate domain heterogeneity. The paper systematically reviews recent advances in DA for agricultural imagery, particularly its practical applications in complex agricultural environments.

We examine the key drivers for adopting DA in agriculture, such as limited labeled data, weak model transferability, and dynamic environmental conditions. We also discuss its use in crop health monitoring, pest detection, and fruit recognition, highlighting improvements in performance across regions and seasons. The paper categorizes DA methods into shallow and deep learning models, with further divisions into supervised, semi-supervised, and unsupervised approaches. A special focus is given to adversarial learning-based DA methods, which have shown great promise in challenging agricultural scenarios.

Finally, we review key public datasets in agricultural imagery, analyzing their value and limitations in DA research. This review provides a comprehensive framework for researchers, offering insights into current research gaps and supporting the advancement of DA methods in agricultural image analysis.

1. Introduction

In agricultural image analysis, the high heterogeneity of data acquisition environments and the extreme scarcity of annotated data severely limit the generalization capability of models across different application scenarios. Among these challenges, the domain shift problem—referring to distribution discrepancies between source and target data—has emerged as a core obstacle hindering the deployment of agricultural intelligent vision systems[1, 2]. To address this, domain adaptation (DA) techniques have been widely introduced into agricultural image analysis in recent years, aiming to enhance model robustness and transferability across cross-regional, cross-temporal, and cross-device data.

Agricultural image data acquisition typically relies on multiple sensors (e.g., RGB cameras, near-infrared cameras, hyperspectral sensors) and is susceptible to complex environmental factors such as illumination variations, seasonal changes, crop varieties, and soil backgrounds. These differences lead to significant distribution shifts for the same agricultural task across datasets, causing models trained under conventional paradigms to suffer drastic performance degradation in new environments[3]. For instance, models trained in laboratories or demonstration farms often exhibit

sharp accuracy drops when deployed in actual fields, different regions, or across growing seasons.

Moreover, annotating agricultural images requires expertise from agronomists and plant protection specialists, resulting in high costs and limited scalability. Compared to general computer vision tasks, the availability of high-quality annotated datasets in agriculture remains extremely scarce[4]. Consequently, directly transferring pre-trained models from natural image domains proves ineffective, underscoring the necessity of domain adaptation to reduce annotation dependency and enhance cross-domain adaptability.

The core of domain adaptation lies in minimizing feature distribution discrepancies between source and target domains, enabling models to achieve comparable performance on the target domain. Recently, DA techniques have demonstrated significant efficacy in key tasks such as crop disease/pest detection, hyperspectral image processing, crop growth monitoring, and precision farming management. Particularly under unsupervised or weakly supervised conditions, their ability to model data distribution shifts positions them as a critical pathway toward scalable agricultural visual intelligence.

Although numerous surveys on transfer learning and domain adaptation exist in natural image analysis[5, 6, 7, 8, 9, 10, 11, 12, 13, 14, 15, 16], systematic reviews tailored to

 242250440@st.usst.edu.cn (S. Chen); dwzhang@usst.edu.cn (D. Zhang)

 huxing@usst.edu.cn (X. Hu)

ORCID(s): 0000-0003-1930-0372 (X. Hu)

agricultural image analysis remain insufficient. Current studies often focus on specific subtasks (e.g., plant disease detection), lacking comprehensive comparisons and analyses of DA methods across agriculture's multitask, multimodal, and multiscenario applications.

To bridge this gap, this review systematically summarizes advances in domain adaptation methods for agricultural image analysis. Existing approaches are categorized into shallow models and deep learning models based on technical pathways, and further subdivided into supervised, semi-supervised, and unsupervised DA methods according to supervision strategies. Additionally, we highlight the extensive application of adversarial learning-based DA strategies in agricultural vision and analyze the impact of domain-specific challenges (e.g., seasonal variations, multi-source data fusion, extreme annotation imbalance) on model design.

This survey aims to consolidate current research and methodological evolution, address systematic gaps in cross-domain modeling for agricultural images, and provide theoretical foundations and methodological references for future domain adaptation technologies in agricultural intelligent perception and autonomous systems.

2. Background

2.1. Domain Shift in Agricultural Image Analysis

In agricultural image analysis, domain shift refers to the changes in data distribution between the training dataset (source domain) and the test dataset (target domain). Domain shift can cause models to perform well on the source domain but fail to generalize effectively to the target domain, thus severely affecting the model's generalization ability. Agricultural image data often exhibits significant distributional differences due to various factors such as environmental variations, crop types, and imaging conditions. Specifically, agricultural images captured in different regions or under varying environmental conditions typically display differences in lighting, climate, seasonal changes, crop varieties, and camera angles, which exacerbate the domain shift phenomenon.

As shown in Figure 1, many researchers have focused on applying domain adaptation methods to address the challenges in agricultural image analysis across a variety of tasks.

For example, in crop classification tasks, agricultural images collected from different regions exhibit significant distributional heterogeneity. Figure 2-2 further illustrates this phenomenon by showing the image-level distribution differences from varying imaging conditions and devices. It becomes evident that domain shift exists within agricultural image data. These issues directly impact the accuracy and robustness of tasks such as crop monitoring and pest detection, especially in cross-regional, cross-seasonal, and cross-device data analysis.

Figure 2 shows aerial images captured during different seasons, with clear differences in lighting and climate between the rainy and dry seasons. These environmental

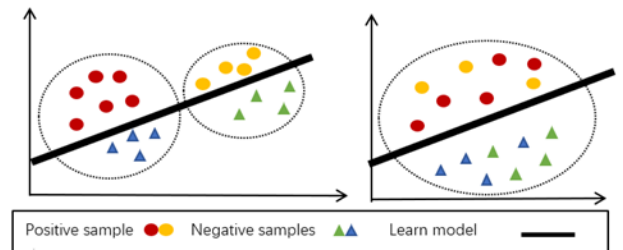


Figure 1: Illustration of source and target data, showing (left) the original feature distribution, and (right) the new feature distribution after domain adaptation. The domain adaptation technique helps alleviate the "domain shift" problem between the source and target domains.



Figure 2: Aerial scenes from Ghaziabad, India, captured during the rainy and dry seasons.

variations result in distributional discrepancies between the source and target domains. As the demand for agricultural image analysis grows, Domain Adaptation (DA) has gradually emerged as one of the key technologies for addressing the domain shift problem. By reducing the distributional differences between the source and target domains, DA methods can enhance the generalization ability of agricultural image analysis models across regions and devices, thereby improving the accuracy and robustness of tasks such as crop classification and pest detection.

2.2. Domain Adaptation and Transfer Learning

In a typical transfer learning (TL) setting, there are two core concepts: "domain" and "task." A domain refers to the feature space of a specific dataset and its marginal probability distribution of features, while a task involves the label space and the target prediction function of the dataset. The goal of transfer learning is to transfer the knowledge learned from task T_a in domain A to task T_b in domain B. It is important to note that during the transfer learning process, either the domain or the task may change. Domain Adaptation (DA) is a special and popular form of transfer learning. In domain adaptation, it is assumed that the feature space and task remain unchanged, while the marginal distributions between the source domain (S) and the target domain (T) differ. This can be mathematically represented as follows: let $X \times Y$ denote the joint feature space and the corresponding label space. The source domain S and the target domain T are defined on $X \times Y$, but their distributions P_S and P_T differ. Suppose there are n_s labeled samples in the source domain $D_S = \{(x_i^S, y_i^S)\}_{i=1}^{n_s}$ and n_t samples (possibly labeled or unlabeled) in the target domain $D_T = \{(x_j^T)\}_{j=1}^{n_t}$. The goal of domain adaptation is to transfer the knowledge learned from the source domain S to the target domain T for performing a specific task that is common to both domains. Domain adaptation works by reducing the distribution difference between the source and target domains, which allows models to better adapt to the target domain data, thereby improving performance and robustness in agricultural image analysis tasks.

2.3. Domain Adaptation Problem Setup

In the agricultural domain, domain adaptation methods primarily face the challenge of significant discrepancies between the source and target domains, which are particularly manifested in spatial distribution, temporal sequences, and modality diversity of the data. Agricultural data are typically collected from heterogeneous sources such as satellite remote sensing, unmanned aerial vehicle (UAV) imagery, and ground sensors. Variations in climate conditions, crop types, and sensor characteristics across different environments lead to substantial distribution heterogeneity among agricultural image datasets. To enhance model generalization in cross-domain agricultural image analysis, domain adaptation techniques have emerged as key solutions by bridging the distribution gap between domains. According to the availability of labels in the target domain, existing methods can be categorized into unsupervised, semi-supervised, and supervised domain adaptation, with unsupervised domain adaptation (Unsupervised DA) attracting particular research interest due to the scarcity of annotated target domain data.

Early domain adaptation research focused mainly on aligning distributions between source and target domains, adopting three technical paths: instance-based alignment (e.g., sample reweighting), feature space mapping (e.g., subspace learning), and classifier parameter adaptation. These methods typically rely on handcrafted feature extractors and aim to reduce domain discrepancy via statistical matching

or weight adjustment strategies. For instance, instance-based methods enhance relevance by reweighting source samples; feature-based methods align feature spaces through linear projections; classifier-based methods improve adaptability through parameter regularization. Given their foundation in traditional machine learning frameworks, these approaches boast low algorithmic complexity, high training efficiency, and strong interpretability, making them especially suitable for resource-constrained agricultural scenarios. Therefore, we collectively term these techniques shallow domain adaptation (Shallow DA), as they depend on shallow features and lightweight models.

In 2014, Girshick et al. [17] introduced R-CNN in a conference paper, pioneering the use of convolutional neural networks (CNNs) for image feature extraction and opening the door to deep learning-based object detection. Building on R-CNN, Girshick proposed Fast R-CNN [18], addressing the inefficiency caused by numerous overlapping region proposals. Subsequently, Ren et al. presented Faster R-CNN in 2016 [19], integrating feature extraction, bounding box regression, and classification into a unified end-to-end network, significantly improving detection accuracy and speed. Fuentes et al. [20] applied a Faster R-CNN framework combined with VGGNet/ResNet to localize tomato disease and pest regions, achieving a mean Average Precision (mAP) of 85.98% over 10 disease classes, marking the widespread adoption of Faster R-CNN in plant disease detection. Given their reliance on complex models and deep feature learning, such methods are categorized as deep domain adaptation (Deep DA).

In summary, domain adaptation methods can be systematically divided into two paradigms: traditional shallow methods and modern deep methods. Shallow approaches mainly encompass classic algorithms based on instances, features, and classifiers, while deep methods are further subdivided into unsupervised, semi-supervised, and supervised categories based on target label usage (see Table 2-1). These two paradigms complement each other in computational efficiency, adaptability, and application scenarios, providing a multi-level solution framework for cross-domain agricultural image analysis.

3. Shallow DA Methods

In this section, we review shallow domain adaptation (DA) methods based on manually engineered features and traditional machine learning models used in agricultural data analysis. Shallow DA methods mainly include three common strategies: 1) instance weighting, 2) feature transformation, and 3) classifier-based adaptation.

3.1. Instance Weighting

Instance weighting is one of the widely adopted shallow domain adaptation strategies in agricultural data analysis. Instance-based DA methods primarily adjust the marginal distribution of source or target samples to ensure consistency in the domain distribution. Let $p_t(x)$ and $p_s(x)$ represent the marginal density distributions of the source and target

Table 1
Classification of DA Methods

CATEGORY	SUBCATEGORIES	TYPICAL EXAMPLES
Shallow DA	Instance-based	DIAFAN-TL, RHM, HSI, CSSPL
	Feature-based	SA, TSSA, ECMDCM, CropSTGAN, MultiCropGAN, Spatial-Invariant Features, Invariant Features in RKHS, Sensor-driven Hierarchical DA, PSO-TrAdaBoost, ESMSL, HSL-GM
	Classifier-based	MLCA, BCC, SSGF, MDAF, WRF, CDELM, BHC, DASVM, SD-AL, AMKFL, VSV, EasyTL
Deep DA	Semi-supervised learning	MAML, WheatSeedBelt, SSDA-WheatHead, SSDA-WheatSeg, TDA-YOLO, SCDAL, CDADA
	Unsupervised learning	MSFF, GAN-DA, Standard GAN, DeepDA-Net, U-DA-Net, Tri-ADA, MaxEnt-DA, DAE-DANN, Self-Attn-DA, ADANN, OpenDA, AdaptSegNet, ADVENT, BDL, DFENet, TSAN, DAN, WDGR, CORAL, Transformer-UDA, MRAN, WPS-DSA, NCADA, TCANet, DDA-Net, TDDA, TST net, AMF-FSL, MSUN, MSCN, AMRAN, DJDANs, CLA

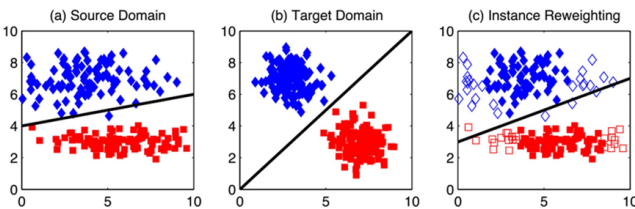


Figure 3: Illustration of instance weighting to alleviate domain shift. (a) The source domain after feature matching (i.e., shared feature representations are discovered by jointly reducing distribution discrepancies and preserving important attributes of the input data). (b) The target domain after feature matching. (c) The source domain after the joint application of feature matching and instance weighting, where the unfilled markers represent irrelevant source instances with smaller weights. Image provided by Long et al. [21]

samples, respectively. The importance weight can be defined as:

$$w(x) = \frac{p_t(x)}{p_s(x)} \quad (1)$$

In this method, source domain samples are assigned different weights based on their relevance to target domain samples. More relevant source samples, such as crop observation data from neighboring regions, are given higher weights, thereby reducing the discrepancy between the source and target domains. Training a model (e.g., classifier or regressor) on the re-weighted source samples can effectively minimize the distribution difference between the two domains. For example, as shown in Figure 3, instance weighting significantly reduces the gap between the source and target domains. This change is clearly observable when comparing Figure 3 (a) with Figure 3 (b).

Molina-Cabanillas et al. [22] proposed a novel instance-weighted transfer learning algorithm, DIAFAN-TL (Domain-Invariant Agricultural Features Adaptation Network for Transfer Learning), applied to phenological prediction across

multiple olive tree cultivars. By dynamically weighting samples based on their relevance between source and target domains, the method enhances information diversity while mitigating sample inconsistency. Yaras et al. [23] introduced a Random Histogram Matching (RHM) approach, which significantly improves satellite image domain adaptation through data augmentation. They systematically analyzed causes of domain shift (e.g., sensor parameter discrepancies, illumination fluctuations, and imaging environment variations), modeled these factors as nonlinear pixel transformations, and leveraged deep neural networks to augment training data, thereby enhancing model robustness against distribution shifts.

For migration framework optimization, Cui et al. [24] developed an Iterative Weighted Active Transfer Learning (IWATL) framework for hyperspectral image (HSI) classification. By dynamically adjusting source domain sample weights via a dual-evaluation mechanism, this framework substantially improves classification accuracy for agricultural HSI. Li et al. [25] proposed a Cost-Sensitive Self-Paced Learning (CSSPL) framework that employs hybrid weight regularization to intelligently allocate multi-temporal image samples, effectively addressing temporal variation challenges in agricultural monitoring.

Within the domain adaptation methodology, instance-based adaptation strategies focus on a two-stage optimization: first aligning data distributions through sample re-weighting and feature selection, then integrating the optimized feature representations with enhanced classifiers. Such compound strategies have been proven to significantly boost feature transferability and classifier generalization in agricultural remote sensing scenarios.

3.2. Feature Transformation

Feature-based domain adaptation methods map source and target domain data to a shared feature representation space using techniques such as subspace alignment, manifold learning, or low-rank representations. These methods aim to eliminate the distribution discrepancy between the

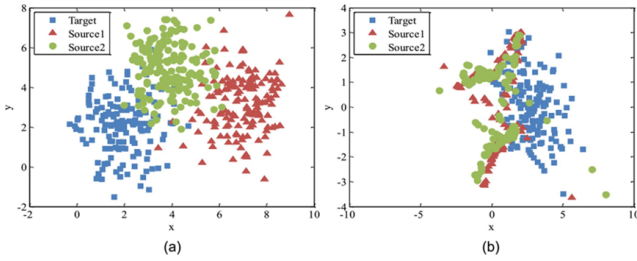


Figure 4: Illustration of feature transformation to reduce domain shift. Each color represents a specific domain. (a) Data distributions of two source domains and one target domain before feature transformation, and (b) data distributions after feature transformation. Image provided by Wang et al. [27].

two domains during joint feature extraction [26]. The approach first constructs a new feature space with domain invariance, as shown in Figure 4. Then, a classifier is trained based on the transformed source domain features and their labels, ultimately enabling effective prediction of target domain samples. Typical implementation strategies include subspace-based projection reconstruction and nonlinear transformation-based feature re-encoding. The core goal is to make cross-domain data distributions more consistent through feature space transformation, thereby enhancing the model’s generalization performance on the target domain.

3.2.1. Subspace-Based Adaptation

Subspace-based domain adaptation (DA) methods typically project source and target samples into separate subspaces using subspace learning or dimensionality reduction techniques, and then align the subspaces. The Subspace Alignment (SA) method proposed by Fernando et al. [28] has been extended to multispectral agricultural image classification tasks. By using Principal Component Analysis (PCA), the method aligns the crop spectral feature subspaces from different seasons, thereby alleviating domain shift caused by variations in lighting and growth stages. In this way, the SA method effectively mitigates differences due to seasonal and lighting variations in agricultural image domain adaptation, enhancing the model’s adaptability and classification performance. The process of SA is shown in Figure 5.

As shown in the figure, the source domain samples $X_s \in R^{n_s \times D}$ consist of n_s samples, each with d -dimensional features. The target domain samples $X_t \in R^{n_t \times D}$ also consist of n_t samples, with the same dimensionality as the source domain data. PCA is used to generate the source and target subspaces, which are then aligned using a linear transformation matrix M .

This method first uses Principal Component Analysis (PCA) to generate a single subspace for both the source and target domains, and then learns a linear transformation matrix M to align these subspaces. The core formula for subspace alignment is:

$$M = \underset{M}{\operatorname{argmin}} \| P_s M - P_t \|_F^2 = P_s^T P_t \quad (2)$$

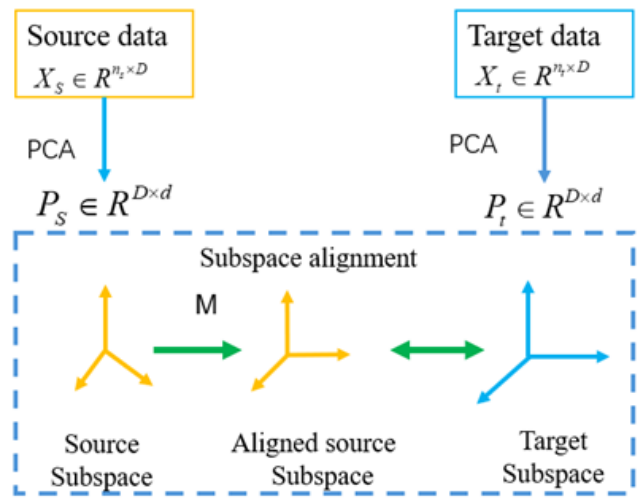


Figure 5: Illustration of Subspace Alignment.

This formula represents the minimization of the distribution discrepancy between the source and target domains through the linear transformation matrix M . Specifically, P_s and P_t represent the feature matrices of the source and target domains, respectively. The matrix M is the optimization target, which transforms the feature space of the source domain so that the features of both domains are aligned as much as possible, thereby reducing their distributional differences. Here, $\| \cdot \|_F^2$ represents the Frobenius norm, which is the square root of the sum of the squares of the matrix elements, and it is used to measure the difference between the two domains after the transformation. Sun et al. [29] directly applied Subspace Alignment (SA) to cross-view scene classification by using Partial Least Squares (PLS) to construct a shared discriminative subspace between the source and target domains. This method effectively captures the common spectral features of crops under different sensors, improving the cross-platform identification accuracy of staple crops such as wheat and rice. They further proposed the Transfer Sparse Subspace Analysis (TSSA) algorithm for unsupervised cross-view remote sensing scene classification [30]. By minimizing the Maximum Mean Discrepancy (MMD) through sparse subspace clustering, TSSA retains the self-expressive characteristics of data at different maize growth stages, achieving classification of crop conditions across growth periods. Weilandt et al. [31] proposed the Early Crop Mapping based on Dynamic Clustering Method (ECMDCM), introducing a novel dynamic clustering method that uses time-series NDVI and EVI data to improve the accuracy of early crop mapping. This method demonstrates significant improvements over traditional static clustering techniques, providing more dynamic and accurate crop type mapping. Li et al. [32] introduced the CropSTGAN framework to address the challenge of cross-domain variability in remote sensing-based crop mapping. This framework includes a domain mapper that effectively adjusts different geographic and temporal

scales, even in the presence of significant data distribution differences. Wang et al. [33] developed the MultiCropGAN framework to address domain transfer and label space differences, which are commonly found in global agricultural environments. By incorporating identity loss into the generator's loss function, MultiCropGAN ensures the retention of key data features, enhancing authenticity and improving the accuracy of crop type classification. The method was extensively tested in northern regions of the Americas, highlighting its effectiveness, especially in handling differences in label space, thereby improving the reliability and applicability of crop mapping technologies. Adversarial learning methods based on category mapping provide another perspective for feature alignment. Takahashi et al. [34] proposed category-information-guided feature space alignment, mapping both source and target domains to a shared category semantic space via adversarial training. This method effectively solves domain shift issues in agricultural images caused by differences in acquisition devices and environmental conditions. It does not require labeled data from the target domain but uses source domain category labels to constrain feature distribution similarity, significantly improving accuracy in object recognition and segmentation tasks across different crop types and field environments. Feature-invariant methods can be considered a special case of subspace-based adaptation. They aim to select a set of features that are unaffected by variations in the data. These selected features can form a new subspace. Bruzzone et al. [35] proposed a multi-objective optimization framework for selecting spatially invariant features to classify non-overlapping scenes. The multi-objective framework ensures that the selected features have high discriminability and high spatial invariance. Invariant feature selection can also be performed in Reproducing Kernel Hilbert Spaces (RKHS) [36]. Paris et al. [37] proposed a sensor-driven hierarchical DA method based on invariant features. Yan et al. [38] introduced TrAdaBoost, based on an improved Particle Swarm Optimization (PSO) method, for cross-domain scene classification, which can select the optimal feature subspace for instance classification. To address the challenges faced in hyperspectral image classification in agricultural remote sensing—such as misclassification caused by inconsistencies between label information and spectral feature space definitions, as well as high computational complexity and inefficiency in similarity learning with large-scale data—Yi [39] proposed an innovative method based on set similarity metric subspace learning. Experiments show that this method improves classification accuracy by 8%-15% compared to traditional subspace methods (such as Linear Discriminant Analysis and Non-Parametric Weighted Feature Extraction) on typical agricultural hyperspectral datasets like Indian Pines and Salinas Valley. It also reduces training time by 40%-60%, demonstrating its comprehensive advantages in efficiency and accuracy and providing a scalable technological path for smart agricultural monitoring. To address cross-domain distribution mismatch problems in multi-temporal remote sensing image classification caused by changes in atmospheric conditions, sensor differences, and a lack of labeled data, Banerjee [40] proposed a hierarchical subspace learning method. The core contribution lies in solving the defects of traditional domain adaptation (DA) techniques, which overlook inter-class semantic similarities and have a coarse global subspace alignment granularity, by using a semantic-driven binary tree structure and Grassmannian manifold subspace alignment. Experiments show that this method improves accuracy by 5%-6% compared to traditional subspace DA methods (such as Global GFK and Subspace Alignment) on datasets like Botswana Hyperspectral and Landsat TM. It significantly reduces misclassification rates when processing semantically similar categories, such as crops in different growth stages, providing an efficient and scalable cross-domain classification solution for remote sensing tasks like disaster monitoring and urban expansion analysis.

atmospheric conditions, sensor differences, and a lack of labeled data, Banerjee [40] proposed a hierarchical subspace learning method. The core contribution lies in solving the defects of traditional domain adaptation (DA) techniques, which overlook inter-class semantic similarities and have a coarse global subspace alignment granularity, by using a semantic-driven binary tree structure and Grassmannian manifold subspace alignment. Experiments show that this method improves accuracy by 5%-6% compared to traditional subspace DA methods (such as Global GFK and Subspace Alignment) on datasets like Botswana Hyperspectral and Landsat TM. It significantly reduces misclassification rates when processing semantically similar categories, such as crops in different growth stages, providing an efficient and scalable cross-domain classification solution for remote sensing tasks like disaster monitoring and urban expansion analysis.

3.2.2. Transformation-based Adaptation

The core goal of transformation-based Domain Adaptation (DA) methods is to reduce the discrepancy between the source and target domains by directly adjusting the distribution of the data or features, rather than relying on subspace projections and alignments. These methods typically use mapping functions to transform the data into a shared feature space, or directly apply transformations at the data level, so that the distributions of both domains align. Aptoula's research [41] provides a crucial framework for domain-adaptive weed and crop classification in agricultural scenarios. The core of this approach lies in using deep learning techniques to enable cross-domain feature sharing, effectively mitigating the data distribution shift caused by differences in lighting, soil conditions, and crop growth stages. This research aligns theoretically with current mainstream transformation-based domain adaptation methods. By mapping the original agricultural remote sensing data into a new representation space, it significantly reduces the statistical (marginal and conditional) and geometric distribution differences between agricultural domains while preserving the underlying structural features. Such methods have shown significant application potential in fields like agricultural remote sensing and crop monitoring (Figure 6).

The core of these methods often utilizes metrics such as Maximum Mean Discrepancy (MMD), Kullback-Leibler Divergence (KL Divergence), or Bregman Divergence to quantify domain distribution differences. In agricultural scenarios, MMD is widely used due to its adaptability to high-dimensional data. It is defined as:

$$MMD(X_s, X_t) = \left\| \frac{1}{n_s} \sum_{\mathbf{x}_i \in X_s} \phi(\mathbf{x}_i) - \frac{1}{n_t} \sum_{\mathbf{x}_j \in X_t} \phi(\mathbf{x}_j) \right\|_F^2 \quad (3)$$

where $\phi(\cdot)$ represents the mapping induced by the kernel function to a Reproducing Kernel Hilbert Space (RKHS), and X_s and X_t represent the source and target domain data, respectively.

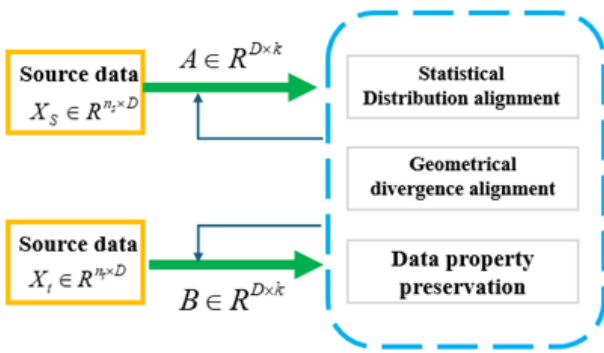


Figure 6: Illustration of Transformation-based Adaptation.

The suitability of different kernel functions in agricultural high-dimensional data (such as hyperspectral images) mainly lies in their ability to perform nonlinear transformations and capture the complex spatial and spectral features in the data. Here is an analysis of different kernel functions:

Linear Kernel: The linear kernel is typically suitable for data with simple, linearly separable features. However, in agricultural high-dimensional data, especially hyperspectral images, spectral features usually exhibit strong nonlinear relationships, meaning the linear kernel may not adequately capture the complex distribution differences between the source and target domains.

Radial Basis Function (RBF) Kernel: The RBF kernel can effectively capture local variations in data through nonlinear mapping, making it particularly suitable for high-dimensional, complex, nonlinear structures in agricultural data. For example, the reflectance values across different bands in hyperspectral images may show complex variations, and the RBF kernel handles these local feature differences well. Therefore, the RBF kernel is widely used in agricultural data, especially when strong nonlinear mappings exist between the source and target domains.

Polynomial Kernel: The polynomial kernel expands the polynomial features of the data, allowing it to accommodate nonlinear distributions to some extent. In hyperspectral data, when there is some correlation between different spectral features, using a polynomial kernel may be an effective choice. However, high-degree polynomial kernels can lead to computational overhead and overfitting issues.

Sigmoid Kernel: The sigmoid kernel mimics the activation function in neural networks and is suitable for capturing specific nonlinear relationships. However, it is rarely used in agricultural high-dimensional data because it may lead to model instability or optimization difficulties, particularly with large datasets.

In summary, the RBF kernel is generally the preferred choice when dealing with agricultural high-dimensional data (especially hyperspectral images). It effectively handles complex nonlinear relationships and high-dimensional features, while also providing reasonable computational efficiency. When selecting a kernel function, it is important

to consider the actual distribution characteristics of the data and available computational resources to ensure the best model performance. To address domain distribution differences, Pan et al.[42] proposed Transfer Component Analysis (TCA), which uses kernel techniques to map the source and target domains into a Reproducing Kernel Hilbert Space (RKHS) and measures the domain distance using MMD. The objective function for TCA is:

$$\min_{W} (W^\top K L K^\top W) + \mu \text{tr}(W^\top W) \quad (4)$$

This method, with its adaptability to growth stages and low annotation requirements, generally improves model performance in cross-domain tasks and provides an expandable technological foundation for pest monitoring, yield prediction, and resource management. Derivatives of Canonical Correlation Analysis (CCA) also perform well in agricultural heterogeneous Domain Adaptation (DA).

These methods, through theoretical innovations and adaptation to agricultural scenarios, provide effective tools to address domain shift issues caused by climate differences, sensor changes, or crop growth stages. This advances the generalization capability of models in smart agriculture.

3.3. Classifier-Based Adaptation

Classifier-based domain adaptation (DA) methods adjust classifier parameters trained on the source domain by leveraging unlabeled samples from the target domain, demonstrating significant utility in agricultural applications. The following approaches offer effective solutions to domain shift challenges in agriculture.

In agricultural scenarios, distribution discrepancies of imagery are often mitigated through dynamic updates of classifier parameters. The maximum likelihood classifier adaptation method proposed by Bruzzone et al. [43, 44, 45, 46] was successfully applied to cross-season crop classification tasks, where classifier parameters are iteratively adjusted to fit the statistical properties of imagery from new seasons. Similarly, an improved Bayesian cascade classifier approach [44] enhanced robustness for cross-regional crop type recognition. Zhong et al. [47] combined spectral-spatial guided filtering with classifier update strategies, significantly improving crop disease detection accuracy under varying farmland environments.

Given the complexity of cross-domain agricultural scenarios, ensemble learning has become a widely adopted technique for improving classification performance and robustness. By integrating predictions from multiple base classifiers, ensemble methods effectively reduce overfitting and bias inherent in single classifiers. In agricultural tasks, ensemble learning leverages multi-classifier voting strategies to strengthen model adaptability and robustness. For example, Wei et al. [48] proposed a Multi-Domain Adaptation Fusion (MDAF) approach that alleviates spectral variability issues across countries' farmland remote sensing classification through an ensemble of classifiers.

Furthermore, weighted classifier transfer based on Random Forests is extensively used in agricultural classification tasks. Zhang et al. [49] employed weighted Random

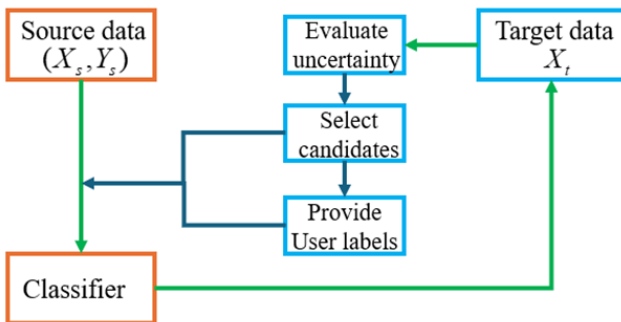


Figure 7: Flow chart of DA's AL method

Forest classifiers to integrate agricultural data from different geographic regions for cross-regional crop disease detection, substantially improving classification accuracy. This method adjusts classifiers on both source and target domains through weighted aggregation, harnessing ensemble learning benefits to boost generalization, particularly in complex and variable agricultural environments. Xu et al. [50] extended Extreme Learning Machine (ELM) parameter transfer to cross-climate crop yield prediction by aligning features across geographical domains with kernel functions, further advancing ensemble learning applications in agriculture.

Considering the high cost of agricultural data annotation, semi-supervised learning (SSL) and active learning (AL) have garnered widespread attention. Rajan et al. [51] introduced a Binary Hierarchical Classifier (BHC) framework integrating SSL, successfully enabling progressive updates for cross-year crop pest and disease monitoring models. The classical Domain Adaptation SVM (DASVM) method, after improvements, was applied to cross-sensor crop classification, achieving notable enhancement in model generalization with minimal labeled target samples [52].

As illustrated in Figure 7, Active Learning (AL) methods initially train a classifier on the source domain data and then classify target domain samples. By selecting samples with the highest prediction uncertainty and obtaining human annotations for them, these samples are incorporated into the training set to iteratively update the classifier. AL techniques have gained considerable attention in precision agriculture due to their efficiency in reducing annotation costs.

For instance, Deng et al. [53] combined active learning with multi-kernel learning to propose an Active Multi-Kernel Domain Adaptation (AMKDA) method, which significantly reduced the annotation requirements for classifying hyperspectral images across different soil types. Kalita et al. [54] developed a standard deviation (SD)-based AL technique that leverages labeled source images to select the most "informative" target samples, improving the effectiveness of sample selection. Saboori et al. [55] introduced Active Multi-Kernel Fredholm Learning (AMKFL), formulating a Fredholm kernel regularization model to guide sample

annotation, thus enhancing target domain classification performance.

The high variability in scale and morphology of agricultural objects has driven the design of novel classifiers. Izquierdo-Verdiguier et al. [56] proposed the Virtual Support Vector (VSV) method, which embeds rotation and scale invariance to achieve up to 12% accuracy improvement in UAV-based farmland image classification. Wang et al. [57] introduced EasyTL, a non-parametric transfer learning approach that enables crop status recognition across growth stages on resource-constrained edge computing devices deployed in fields, demonstrating strong practical applicability and adaptability.

3.4.

sectionSummary of Shallow DA Methods Shallow domain adaptation (DA) methods primarily rely on traditional machine learning techniques and handcrafted features to address distribution differences between the source and target domains. Specifically, common technical approaches include instance weighting, feature transformation, and classifier-based adaptation. Instance weighting methods adjust the weights of source domain samples to reduce distribution differences between the source and target domains, thereby enhancing the model's generalization ability. Feature transformation methods map the source and target domains to a shared feature space, achieving alignment of feature spaces to reduce inter-domain differences. Classifier-based adaptation methods focus on adjusting the classifier parameters to achieve alignment between the source and target domains.

The main advantages of shallow methods lie in their high computational efficiency, ease of implementation, and relatively low demand for computational resources, making them suitable for resource-constrained agricultural applications. However, shallow methods tend to perform poorly when dealing with high-dimensional, complex patterns, and large-scale agricultural data. Their feature representation capabilities and learning complexity are limited. Especially in scenarios with significant distribution differences or high task complexity, shallow methods often fail to capture the deep relationships between the data, thus affecting their practical application in the agricultural field.

4. Deep Domain Adaptation (DA) Methods

With the rapid development of deep learning technologies, domain adaptation (DA) methods based on deep neural networks have shown significant advantages in agricultural data analysis. Deep DA methods automatically extract domain-invariant features through end-to-end feature learning and distribution alignment mechanisms, effectively addressing domain shift problems caused by sensor differences, environmental changes, and varying crop growth stages. Based on the labeling status of the target domain data, deep DA methods can be categorized into supervised, semi-supervised, and unsupervised approaches. This section

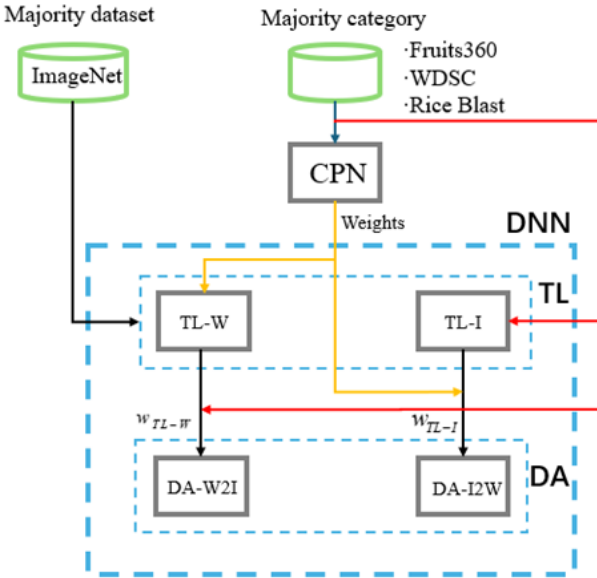


Figure 8: Structure of the method by Takahashi et al. [34].

systematically reviews their core principles and progress in agricultural applications.

4.1. Supervised Deep DA

Supervised deep DA methods assume that there is a small amount of labeled data in the target domain. These methods achieve simultaneous optimization of feature space and classifier by jointly optimizing the source domain classification loss and cross-domain alignment loss. The core idea is to construct a deep network for joint training, using target domain label information to directly constrain the feature distribution alignment process. A typical supervised deep DA model includes a feature extractor, classifier, and domain discrepancy measurement module, optimized by minimizing the following objective function:

$$L = L_{cls}(X_s, Y_s) + \lambda \cdot L_{align}(X_s, X_t) \quad (5)$$

Where $L_{cls}(X_s, Y_s)$ is the source domain classification loss, $L_{align}(X_s, X_t)$ is the cross-domain alignment loss (such as MMD, adversarial loss, or covariance matching), and λ is the balancing parameter.

In agricultural applications, supervised deep domain adaptation (DA) is widely used for cross-sensor data fusion and multi-temporal crop monitoring tasks. For example, Takahashi et al. [34] proposed a category-mapping-based adversarial learning method that incorporates source domain class labels to constrain feature space alignment, thereby enhancing the model's generalization ability to the target domain in agricultural image recognition tasks involving data collected from different devices (see Fig. 8). This supervised domain adaptation approach consists of three main steps: image generation, transfer learning, and domain adaptation based on deep neural networks (DNNs). In the first step, a

Class Propagation Network (CPN) is employed to generate a class map from the target image, aiming to simulate the distribution characteristics of real agricultural imagery. In the second step, transfer learning is conducted on both the real image I and the synthetic image W , resulting in two separate transfer learning models, TL-I and TL-W. In the third step, deep neural networks are used to perform domain adaptation, building two additional derivative models—DA-W2I for adapting synthetic to real images, and DA-I2W for adapting real to synthetic images.

Figure 8 illustrates the overall structure and data flow of the proposed method. The entire architecture comprises five key modules: CPN (image generation), TL-I (transfer learning with real images), TL-W (transfer learning with synthetic images), DA-W2I (domain adaptation from synthetic to real), and DA-I2W (domain adaptation from real to synthetic) [58]. These components work synergistically to improve the model's generalization ability on agricultural target domain data. The approach is especially beneficial in scenarios with limited labeled data, offering a robust strategy through both image-level and feature-level transfer mechanisms.

Similarly, Espejo-Garcia et al. [59] proposed a method combining agricultural transfer learning with Generative Adversarial Networks (GANs) to generate synthetic images, effectively addressing the scarcity of high-quality annotated data in agriculture.

Supervised convolutional neural networks (CNNs) have demonstrated outstanding performance in computer vision segmentation tasks. In agricultural remote sensing, researchers have explored fully supervised CNNs for farmland extraction. Lu et al. [60] introduced an attention mechanism focusing on important features and designed a feature fusion module to extract farmland from remote sensing images. However, low-resolution feature maps in neural networks may lose critical details during upsampling, causing blurred boundaries. To tackle this, Li et al. [61] designed a method to automatically model pixel-wise spatial contextual correlations and employed post-processing to reduce noise, generating clearer boundaries, though their approach did not account for variations in object sizes.

To address this limitation, Shang et al. [62] proposed a multi-scale object extraction method integrating attention mechanisms, enabling adaptive segmentation of agricultural objects with significant scale variations, yielding strong results. Zhang et al. [63] formulated farmland extraction as an edge detection problem and developed a High-Resolution Boundary Refinement Network (HBRNet) to precisely delineate farmland boundaries.

Nonetheless, the practical application of supervised deep domain adaptation (Deep DA) in agriculture remains challenged by the high cost of acquiring annotated target domain data. For instance, in the Cityscapes dataset [64], manually annotating a single natural image takes approximately 1.5 hours. Consequently, much current research focuses on semi-supervised and unsupervised paradigms to meet the real-world scarcity of labeled data in agricultural scenarios.

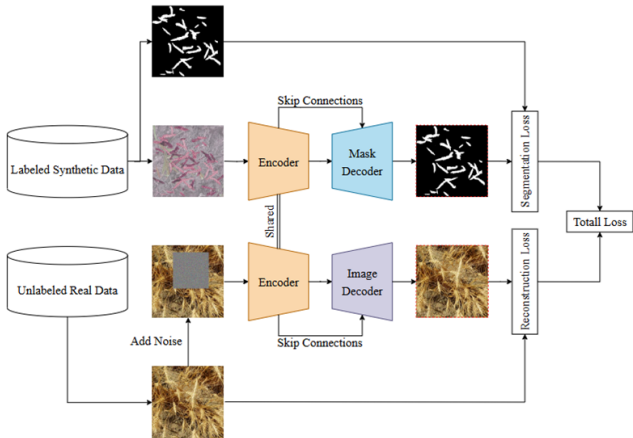


Figure 9: Schematic of the model architecture in Ghanbari's method [65].

4.2. Semi-supervised Deep Domain Adaptation (DA)

Supervised Deep Domain Adaptation (Deep DA) methods leverage fully labeled samples from the source domain along with a small number of labeled or pseudo-labeled samples from the target domain. These methods implement domain transfer through strategies such as self-training, co-training, or hybrid supervision. Their main advantage lies in balancing annotation costs with model performance, making them particularly suitable for agricultural scenarios where labeled target data is scarce.

Self-training and pseudo-label generation are core techniques in semi-supervised DA. Recent innovations have introduced diffusion models into this context with promising results in the agricultural domain. Ghanbari et al.[65] proposed a novel framework that combines diffusion models with meta-learning to address wheat ear segmentation using only a few labeled samples. Specifically, the method requires just three manually annotated wheat images and unlabelled video frames to generate a large pseudo-labeled dataset via a probabilistic diffusion process.

The architecture adopts a dual-branch encoder-decoder network that enables effective feature alignment and semantic consistency between domains (see Fig. 9). The model achieved a Dice score of 63.5% on an external test set comprising farmland images from multiple countries, demonstrating strong generalization capabilities. This diffusion-based pseudo-labeling mechanism significantly enhances the adaptability of deep DA approaches in data-scarce agricultural environments, offering both scalability and practical relevance.

The encoder is designed to learn joint image representations for both synthetic and real images, while the mask decoder generates segmentation masks. Simultaneously, the image decoder reconstructs real images to force the encoder to adapt to real domain characteristics. Experimental results show that this architecture achieves a Dice score of 80.7% on internal test sets and 64.8% on external test sets composed

of images from 18 plots across five countries. These results underscore the framework's potential in developing generalized agricultural vision solutions and promoting the deployment of advanced technologies in real-world scenarios.

By integrating diffusion models, this approach allows the effective use of large-scale unlabeled datasets and has recently demonstrated remarkable progress in image processing tasks [66, 67], further supporting its relevance in precision agriculture applications.

To address the challenges in wheat disease detection, Najafian et al.[68] developed the WheatSeedBelt dataset with a large number of labeled seed images and designed a pipeline combining pretrained models with semi-supervised fine-tuning, achieving high accuracy in FDK classification and questioning the consistency of manual evaluation. To overcome the bottleneck of large-scale annotation, they later proposed a semi-self-supervised wheat head detection method [69], using a small number of annotated images and video sequences to create pseudo-labeled datasets, further enhanced via domain adaptation techniques (mAP = 0.827).

Moreover, they introduced a hybrid approach leveraging synthetic data and multi-domain adaptation for wheat head segmentation [70]. With only two labeled samples, this model achieved a Dice score of 0.89 on internal datasets, increasing to 0.91 after fine-tuning on diverse external data. This significantly improves model generalizability in label-scarce settings and showcases practical viability in real agricultural deployments.

In the context of vegetable detection, Yang et al.[71] proposed a domain-adaptive YOLOv5-based model named TDA-YOLO for tomato detection in densely planted fields under varying lighting conditions. The model uses neural preset color style transfer to generate a pseudo dataset, narrowing the domain gap. The incorporation of semi-supervised learning and knowledge distillation further improves target domain adaptability. Additionally, the integration of a lightweight FasterNet architecture accelerates inference speed significantly.

Zhu et al.[72] introduced a Semi-supervised Center-based Discriminative Adversarial Learning (SCDAL) approach for domain-adaptive scene classification of aerial imagery, where center loss-guided adversarial learning enhances domain discriminability.

Teng et al.[73] proposed the Classifier-constrained Deep Adversarial Domain Adaptation (CDADA) method. Combining the Maximum Classifier Discrepancy (MCD) framework and deep convolutional neural networks (DCNNs), the model enables semi-supervised cross-domain classification in remote sensing scenarios by aligning feature distributions adversarially.

In summary, semi-supervised domain adaptation approaches leverage limited annotated data to guide feature alignment, reduce annotation costs, and enhance model robustness across diverse agricultural environments. These methods offer viable solutions for multimodal data fusion and stage-aware crop monitoring, both critical in precision farming practices.

4.3. Unsupervised Deep Domain Adaptation (DA)

Unsupervised Deep Domain Adaptation (Unsupervised Deep DA) fully leverages labeled source domain data and unlabeled target domain samples to achieve domain-invariant representation learning through feature space transformation or generative models[74, 75]. These approaches can be categorized into adversarial-based methods, discrepancy-based methods, and self-supervised learning, demonstrating significant value in annotation-scarce scenarios such as agricultural robotics and remote sensing mapping[76].

4.3.1. Adversarial Training

Adversarial training, such as Generative Adversarial Networks (GANs), is widely used in Unsupervised Domain Adaptation (UDA), primarily for distribution matching between the source and target domains. The most famous adversarial training methods are the Domain-Adversarial Neural Network (DANN) and the Gradient Reversal Layer (GRL), which are based on the GAN framework. GANs are a class of deep generative models[77], commonly applied in image synthesis tasks. To generate synthetic images, a corresponding training dataset must be provided. Popular image datasets include faces (CelebA[78]), handwritten digits (MNIST[79]), bedrooms (LSUN[80]), and other object categories (CIFAR-10[81] and ImageNet[82]). After training, the generative model can produce synthetic images that are highly similar to the samples in the training dataset.

GANs consist of two competing neural networks[83]. One of these networks is the generator, which accepts a noise vector as input, where the noise contains random values drawn from a distribution (such as normal or uniform distribution). The goal of the generator is to output samples that are indistinguishable from the real training data. The other network is the discriminator, which takes as input either real samples from the training data or fake samples generated by the generator. The task of the discriminator is to determine the probability that the input sample is real. During training, the generator and discriminator play a minimax game, where the generator attempts to deceive the discriminator, while the discriminator strives not to be deceived by the generator[78]. Using the notation from Goodfellow et al.[77], we define the value function $V(D, G)$ for the minimax game played between the generator and the discriminator:

$$\begin{aligned} \min \max V(D, G) = & \mathbb{E}_{x \sim P_{\text{data}}(x)}[\log D(x)] \\ & + \mathbb{E}_{z \sim P_z(z)}[\log(1 - D(x))] \end{aligned} \quad (6)$$

Here, $X \sim P_{\text{data}}(X)$ samples from the real data distribution, $X \sim P_Z(Z)$ samples from the input noise distribution, $D(x; \theta_d)$ is the discriminator, and $G(z; \theta_g)$ is the generator. As shown in the equation, the goal is to find the parameters θ_d that maximize the log-probability of correctly distinguishing real samples x and fake samples $D(G(z))$, while simultaneously finding the parameters θ_g that minimize the log-probability of $1 - D(x)$. $D(G(z))$ represents the probability that the generated data $G(z)$ is real. If the discriminator correctly classifies fake inputs, then $D(G(z)) = 0$, and the quantity $1 - D(x)$ is minimized. This situation occurs

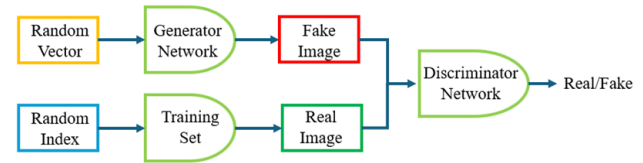


Figure 10: Principle Diagram of GAN Adversarial Training

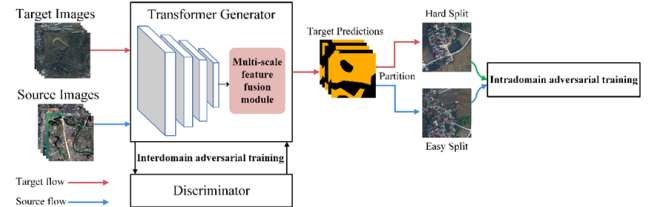


Figure 11: Multi-Scale Cross-Domain Adversarial Training and Feature Fusion Framework by Zhang [85]

when $D(G(z)) = 1$, or when the discriminator incorrectly classifies the generator's output as a real sample. Therefore, the task of the discriminator is to learn to correctly classify inputs as real or fake, while the generator attempts to deceive the discriminator into believing its generated output is real.

In adversarial training, generative adversarial networks (such as Cycle GAN) and discriminative adversarial networks (such as DANN) have different application scenarios and characteristics. Generative adversarial networks (such as Cycle GAN) focus on generating image samples and are commonly used in tasks such as style transfer and image synthesis, while discriminative adversarial networks (such as DANN) focus on feature distribution alignment and are commonly used in feature learning and domain adaptation tasks.

Generative adversarial networks (GANs) typically consist of a generator and a discriminator. The generator learns to generate target domain data samples based on the distribution of source domain data, while the discriminator's task is to determine whether the generated samples belong to the real data of the target domain. In the agricultural domain, GANs are widely applied in image style transfer tasks, especially in cross-sensor image style transfer. For example, Cycle GAN has been applied to cross-sensor style transfer of agricultural remote sensing images, generating the style of source domain images to make them similar to the style of the target sensor, thereby reducing the image differences between sensors[84].

Similarly, Zhang[85] proposed an unsupervised adversarial domain adaptation method for agricultural land extraction. This method helps to reduce the annotation cost of agricultural land remote sensing images by designing a multi-scale feature fusion module (MSFF) that adapts to agricultural land datasets with different spatial resolutions and learns more robust domain-invariant features.

Ji et al.[86] proposed an end-to-end domain adaptation (DA) method based on Generative Adversarial Networks (GANs) for land cover classification from multi-source images. In this approach, source images are transformed into the style of target images through adversarial learning, and a fully convolutional network (FCN) is trained for semantic segmentation of the target images. Tasar et al.[87] introduced a multi-source DA method, known as Standard GAN, for semantic segmentation of very high-resolution (VHR) satellite images. They further designed an unsupervised, multi-source, multi-target, and lifelong DA method for satellite image semantic segmentation. Wittich et al.[88] deployed a deep adversarial DA network for classifying aerial images using semantically consistent appearance adaptation and developed a Color Map GAN for DA in image semantic segmentation. Liu et al.[89] proposed an unsupervised adversarial DA network for agricultural scene classification, where a GAN-based feature extractor brings the source and target distributions closer together, and a classifier trained on the transferred source domain features achieves better classification accuracy in the target domain.

Generative adversarial networks perform excellently in style transfer, converting source domain images to the style of the target domain without paired samples, making them suitable for tasks with large image data differences. However, generative networks are prone to the mode collapse problem, where the generated images lack diversity, and the training process demands substantial computational resources.

Discriminative Adversarial Networks (DANN) use a discriminator to determine whether an input sample comes from the source or target domain. Through backpropagation, the model adjusts the distribution of features in the source and target domains, making them more aligned in feature space, thereby improving the model's generalization ability in the target domain. In the agricultural domain, DANN is commonly used for feature distribution alignment, especially in feature learning and domain adaptation tasks. In this regard, Yan et al.[90] proposed a Tri-ADversarial Domain Adaptation (TriADA) method for pixel-level classification of very high-resolution (VHR) remote sensing images. This method learns a domain-invariant classifier through a domain similarity discriminator. Wang et al.[91] proposed a feature alignment method based on Adversarial Domain Adaptation (ADDA) to address the cross-device calibration problem in hyperspectral imaging systems (such as sensor models and lighting conditions). Through adversarial training, the model eliminates spectral distribution differences between different sensors (e.g., HySpex and Headwall), enabling calibration transfer without standard samples. Experiments conducted on maize plant data collected by two hyperspectral sensors showed a 21.5% reduction in the root mean square error (RMSE) for cross-system prediction of relative water content (RWC), demonstrating the effectiveness of adversarial learning in agricultural phenotype cross-platform model transfer.

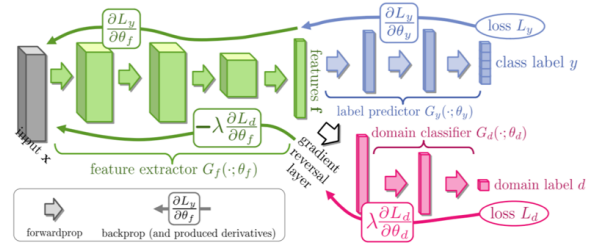


Figure 12: Basic Network Diagram of DANN

Discriminative adversarial methods have also been applied to other domain adaptation (DA) tasks in agricultural imagery. Bejiga et al.[92] proposed a Domain-Adversarial Neural Network (DANN) for large-scale land cover classification from multispectral images. The network consists of a feature extractor, class predictor, and domain classifier block, effectively handling large-scale land cover classification tasks. Rahhal et al.[93] introduced an adversarial learning method for multi-source remote sensing data domain adaptation. This method aligns the source and target domain distributions using a min-max entropy optimization approach. Elshamli et al.[94] employed denoising autoencoders (DAE) and DANN to address the DA problem in multi-spatial and multi-temporal agricultural images. Mauro et al.[95] developed a self-attention-based domain adversarial network for land cover classification from multi-temporal satellite images, where the deep adversarial network reduces domain discrepancies across different geographic regions. Mateo et al.[96] investigated a cross-sensor adversarial DA method for cloud detection using Landsat-8 and Proba-V images. Ma et al.[97] proposed an Adaptive Domain-Adversarial Neural Network (ADANN) to align vegetation indices and meteorological features across different agricultural regions in the U.S. Experimental results showed that the method reduced the RMSE to 0.87 t/ha in cross-state yield prediction, achieving a 34.1% error reduction compared to traditional machine learning methods and validating the transferability of adversarial learning in large-scale agricultural forecasting.

Discriminative adversarial networks can effectively align the feature distributions of source and target domains, improving the accuracy of cross-domain tasks. Especially in cases with scarce labeled data, they can significantly enhance target domain performance with only a small amount of labeled data. However, discriminative adversarial networks rely on precise feature extraction, and large domain discrepancies between source and target may cause training instability or alignment failure.

Adversarial DA methods have wide applications in agriculture, including atypical GAN/DANN adversarial approaches or hybrid strategies, primarily focusing on remote sensing tasks such as scene classification[84], crop classification[98], road extraction[83], and cloud segmentation[99]. However, predefined single distance functions often struggle with different remote sensing datasets.

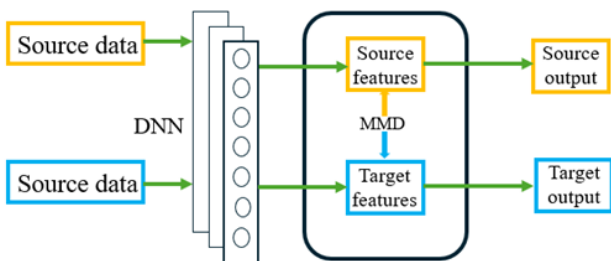


Figure 13: Flowchart of Discrepancy-Based Deep DA Methods

Adversarial domain adaptation can implicitly reduce the distribution differences between data from different domains. Hoffman et al.[100] first introduced adversarial domain training into pixel-level unsupervised domain adaptation. Tsai et al.[101] proposed an adversarial training method (AdaptSegNet), treating segmentation as structured output and reducing domain differences at the output level. Vu et al.[102] proposed an entropy-based method (ADVENT) that converts probability predictions into entropy and uses entropy as the adversarial loss for the network. Li et al.[103] proposed a bidirectional training method (BDL) to align features between source and target domains. Zhang et al.[104] introduced a Domain Feature Enhancement Network (DFENet), which strengthens the discriminative power of learned features to address domain variance in scene classification. Specifically, DFENet explicitly models the channel and spatial dependencies of each domain to recalibrate global and local features. Zheng et al.[105] proposed a two-stage adaptive network (TSAN) for remote sensing scene classification, considering both single-source and multi-target domains. Rahhal et al.[93] proposed a multi-source adversarial DA method based on the min-max entropy optimization approach for source and target domain alignment. Makkar et al.[106] used adversarial learning to extract discriminative target domain features consistent with the source domain for geospatial image analysis.

Saito et al.[107] proposed an approach for open-set domain adaptation scenes that leverages adversarial training to extract features distinguishing known and unknown target samples. During training, the feature generator is given two options: align target samples with source known samples or reject them as unknown target samples.

4.3.2. Discrepancy-Based Alignment

Discrepancy-based deep domain adaptation (DA) methods primarily aim to match the marginal and/or conditional distributions between domains by adding adaptation layers (e.g., MMD-based metrics) in deep neural networks (DNNs)[108], thereby enabling task-specific representations, as shown in Figure 12.

Long et al.[109] proposed a novel Deep Adaptation Network (DAN) architecture that extends deep convolutional neural networks to domain adaptation scenarios. This is the first time that deep neural networks (DNNs) have

been used to learn transferable cross-domain features for domain adaptation. Baktashmotagh et al.[110] introduced a domain-invariant projection method based on the Maximum Mean Discrepancy (MMD) to extract domain-invariant features. Shen et al.[111] proposed a Wasserstein Distance Guided Representation Learning (WDGRL) method, using the Wasserstein distance as a data distribution discrepancy measure. Sun et al.[112] extended CORAL to learn a non-linear transformation (Deep CORAL) to align activation correlations in deep neural network layers.

To address the challenges of limited labeled data and poor generalization of cross-farm crop row detection models in agriculture, Ferreira[113] proposed a visual Transformer framework based on Unsupervised Domain Adaptation (UDA). Through domain difference-driven feature alignment and expansion label simplification strategies, the framework significantly improved the cross-domain robustness of crop row and gap detection. Experiments showed that the Transformer-based SegFormer outperformed traditional convolutional networks (e.g., PSPNet, DeepLabV3+) even without UDA, and the performance was further enhanced after introducing DAFormer, particularly in complex scenarios such as curved rows and shadow interference. This work is the first to combine visual Transformers with UDA for agricultural applications, providing an efficient solution for cross-farm crop monitoring with low labeling costs, thereby advancing the practical use of automated detection technologies in precision agriculture.

Takahashi et al.[34] proposed aligning the source and target domain feature spaces through category mapping, improving agricultural image recognition and segmentation accuracy and addressing the issue of unlabeled data in the target domain. Based on DAN, Long et al.[114] introduced a Multi-Representation Adaptation Network (MRAN)[115] that performs cross-domain classification tasks via multi-representation alignment. They further proposed a Deep Sub-domain Adaptation Network (DSAN)[116], which utilizes sub-domain adaptation principles.

Most previous methods assume that the training and testing sets of High-Resolution Satellite (HSR) images follow the same feature distribution, but in practice, there are often differences in region, resolution, scale, and style between the training and testing sets, leading to diverse feature distributions[117]. Zhu et al.[118] developed a Weak Pseudo-Supervised Decorrelation Sub-domain Adaptation (WPS-DSA) network to address these distribution shifts in cross-domain land-use classification.

To address the issue of data distribution discrepancies caused by environmental factors in field cotton boll status recognition, Li[119] proposed an Unsupervised Domain Adaptation method based on Neighborhood Component Analysis (NCA), called NCADA. This is the first unsupervised domain adaptation application in cotton boll recognition, and it established the first field cotton boll benchmark dataset. The method demonstrated the feasibility of automating the process to replace traditional manual observation, offering a new tool for precision agricultural management



Figure 14: Example Images from the Field Cotton Boll (IFCB) Dataset

and achieving recognition performance superior to traditional classification models and state-of-the-art methods in cross-domain scenarios. Garea et al.[120] proposed a network based on Transfer Component Analysis (TCA) (TCANet) for domain adaptation (DA) of hyperspectral images (HSI), which uses TCA to construct an adaptation layer. Ian et al.[77] introduced a deep DA network (DDA-Net) for cross-dataset HSI classification, which minimizes domain differences and transfers task-related knowledge from the source domain to the target domain in an unsupervised manner. Li et al.[121] proposed a two-stage deep DA (TDDA) method, where in the first stage, the distribution distance between domains is minimized by using Maximum Mean Discrepancy (MMD) to learn deep embedding space, and in the second stage, a spatial-spectral twin network is constructed to learn discriminative spatial-spectral features and further reduce distribution differences. Zhang et al.[122] proposed a Topology Structure and Semantic Information Transmission Network (TST Net), which uses graph structures to describe topological relationships and combines Graph Convolutional Networks (GCN) with Convolutional Neural Networks (CNN) for cross-scene HSI classification. Wang et al.[123] proposed a Graph Neural Network (GNN)-based DA method for multi-temporal HSI, which integrates domain and class CORAL into the GNN network to align the joint distribution of domains. Liang et al.[124] proposed an attention-based multi-source fusion method for deep few-shot learning (AMF-FSL) for small HSI classification, consisting of three modules: target-based class alignment, domain attention allocation, and multi-source data fusion. This method can transfer classification learning capability from multiple source data to target data.

Yan et al.[125] proposed a framework for cross-species plant disease recognition using Unsupervised Domain Adaptation (UDA), which adopts a hybrid sub-domain alignment method to address the classification task of plant disease severity. Fuentes et al.[126] proposed a DA method for tomato disease classification that can handle environmental changes. However, both methods directly applied existing UDA for plant disease classification, without considering the unique challenges posed by cross-species plant diseases. To address this, Wu[127] proposed a novel multi-representation sub-domain adaptation network with uncertainty regularization (MSUN) for field plant disease recognition. This method effectively resolves the uncertainty issues of cross-species multiple diseases, which existing UDA methods fail to address (e.g., large domain differences, large class

differences within domains, and unclear class boundaries within domains).

Othman et al.[128] proposed a DA network for cross-scene classification, which uses pretraining and fine-tuning strategies to ensure that the network can correctly classify source samples, align source and target distributions, and preserve the geometric structure of target data. Similarly, Lu et al.[129] introduced a Multi-Source Compensation Network (MSCN) for cross-scene classification tasks. In this network, cross-domain alignment modules and classifier compensation modules are designed to reduce domain shifts and align categories across multiple sources. Zhu et al.[130] proposed an attention-based Multi-Scale Residual Adaptation Network (AMRAN) for cross-scene classification, which includes a residual adaptation module for marginal distribution alignment, an attention module for robust feature extraction, and a multi-scale adaptation module for multi-scale feature extraction and conditional distribution alignment. Geng et al.[131] proposed a Deep Joint Distribution Adaptation Network (DJDANs) for transfer learning in SAR image classification, which develops marginal and conditional distribution adaptation networks.

Self-supervised learning (SSL) has made significant progress in recent years, particularly in scenarios without labeled data, showing strong feature learning capabilities[132]. For example, Zhao et al.[133] proposed a self-supervised contrastive learning approach (CLA) for leaf disease recognition, which combines self-supervised pretraining and domain adaptation (DAL) fine-tuning in two stages to effectively address the limitations of traditional methods that rely on large-scale labeled data. In the self-supervised pretraining stage, CLA uses a large number of unlabeled, distribution-confused image data to train an encoder through contrastive learning, thereby learning effective visual features. The optimization goal of this stage is similar to the contrastive loss in SimCLR, maximizing the similarity between positive sample pairs and minimizing the similarity between negative sample pairs.

In the fine-tuning stage, CLA uses a small amount of labeled data and aligns the features of labeled and unlabeled data through a Domain Adaptation Layer (DAL), generating more generalized visual representations. The optimization goal of the fine-tuning stage can be expressed as the following formula:

$$L_{DAL} = L_{supervised} + \lambda L_{MMD} \quad (7)$$

In this method, $L_{supervised}$ represents the standard supervised learning loss, and L_{MMD} is the domain alignment loss based on the Maximum Mean Discrepancy (MMD) metric, with λ being the hyperparameter that balances the two loss terms.

Experimental results show that CLA significantly outperforms the comparison methods in both domain adaptation and accuracy, achieving the highest accuracy of 90.52% in the experiments. Additional experiments were conducted to explore the influencing factors of CLA, which helped better understand its working mechanism.

This method innovatively combines self-supervised contrastive learning with domain adaptation, effectively improving the generalization ability and accuracy of leaf disease recognition based on large-scale unlabeled data, thus overcoming the reliance on large amounts of labeled data in traditional methods. In agricultural image analysis, self-supervised contrastive learning reduces domain shift in cross-domain feature alignment tasks, enabling the model to perform more robustly under different environments and conditions, thereby enhancing the model's performance in agricultural applications.

Experimental results show that CLA significantly outperforms the comparison methods in both domain adaptation and accuracy, achieving the highest accuracy of 90.52% in the experiments. Additional experiments were conducted to explore the influencing factors of CLA, which helped better understand its working mechanism.

This method innovatively combines self-supervised contrastive learning with domain adaptation, effectively improving the generalization ability and accuracy of leaf disease recognition based on large-scale unlabeled data, thus overcoming the reliance on large amounts of labeled data in traditional methods. In agricultural image analysis, self-supervised contrastive learning reduces domain shift in cross-domain feature alignment tasks, enabling the model to perform more robustly under different environments and conditions, thereby enhancing the model's performance in agricultural applications.

4.4. Summary of Deep Domain Adaptation (DA) Methods

With the rapid development of deep learning technologies, deep domain adaptation (DA) methods have demonstrated significant advantages in agricultural image analysis. These methods, utilizing deep neural networks (DNNs) and adversarial training, are capable of automatically learning domain-invariant feature representations, effectively addressing the complex problem of domain shift. Typically, deep DA methods are classified into supervised, semi-supervised, and unsupervised categories.

In supervised deep DA methods, source domain classification loss and cross-domain alignment loss are jointly optimized to align the feature distributions between the source and target domains, thereby improving the model's generalization ability in the target domain. Semi-supervised deep DA methods combine fully labeled data from the source domain with a small amount of labeled data from the target domain, balancing labeling costs with model performance, making them particularly suitable for agricultural scenarios with limited labeled data. Unsupervised deep DA methods rely entirely on labeled data from the source domain and unlabeled data from the target domain, achieving domain adaptation through feature alignment or generative models. These methods have a wide range of applications.

The primary advantage of deep DA methods lies in their ability to handle high-dimensional, complex agricultural data and, through end-to-end learning, automatically extract

deep features. This enables them to effectively mitigate domain shifts caused by differences in sensors, environmental changes, and crop growth stages. However, deep DA methods also present certain challenges, including high computational resource demands, long model training times, and poor model interpretability. These issues can be limiting factors in agricultural environments with limited resources or high real-time performance requirements. Nonetheless, with continuous technological advancements, deep DA methods are poised to play an increasingly important role in precision agriculture and smart farming.

5. Experimental Results and Analysis

To effectively demonstrate the superiority of deep domain adaptation (DA) in agricultural applications, this study presents experimental results on plant disease detection, crop yield prediction, and remote sensing image agricultural land extraction. The performance of deep DA is evaluated using both visual results and quantitative metrics.

5.1. Experimental Results, Performance Evaluation, and Various Metrics

OA (Overall Accuracy): The ratio of correctly classified samples to the total number of samples in the test set.

AA (Average Accuracy): The average of the classification accuracy calculated separately for each class.

Kappa Coefficient: A metric that measures the consistency between the classification results and true labels, subtracting the "false consistency" caused by random guessing.

Precision: The ratio of true positive samples for a given class among the samples predicted to belong to that class by the model.

Recall: The ratio of true positive samples for a given class that were correctly predicted by the model, among all actual samples of that class.

F1 Score: The harmonic mean of precision and recall, reflecting both the accuracy and comprehensiveness of the model.

Mean Squared Error (MSE): The average of the squared differences between the predicted and true values. The larger the error, the higher the MSE value.

Root Mean Squared Error (RMSE): The square root of the MSE, which is in the same units as the target variable.

Mean Absolute Error (MAE): The average of the absolute differences between predicted and true values.

Coefficient of Determination (R^2): A measure of how well the model's predictions explain the variance of the true values, ranging from 0 to 1.

Intersection over Union (IoU): The ratio of the overlap between the predicted region and the true region to the union of both regions.

COM: The ratio of correctly predicted agricultural land pixels to the actual agricultural land pixels.

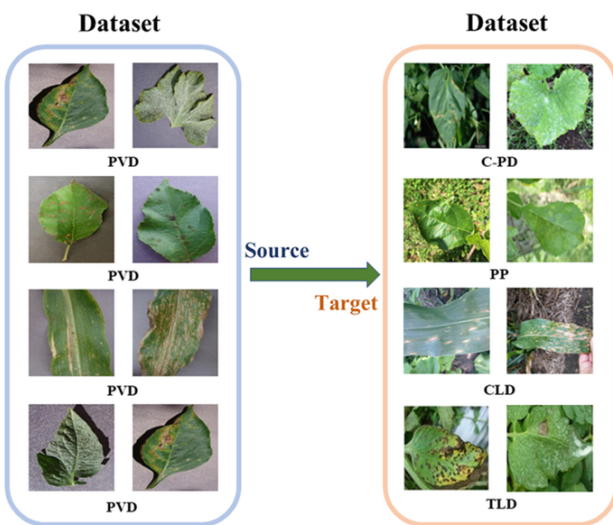
Correctness (COR): The percentage of correctly predicted agricultural land pixels out of all the predicted agricultural land pixels.

F1 Score: The harmonic mean of COM and COR.

Dataset	Resolution	Sensor	Origin Size	Training Data	Test Data
DeepGlobe	0.5m/pixel	Worldview2	2448 x 2448 pixels/image	30,470	N/A
GID	4m/pixel	GF-2	6800 x 7200 pixels/image	73,490	734
LoveDA	0.3m/pixel	Spaceborne	1024 x 1024 pixels/image	15,829	324
PlantVillage	256x256 pixels	RGB	55,000 images	50,000 images	5,000 images
PlantDoc	Variable	RGB	2,500 images	2,000 images	500 images
Plant-Pathology	2048x1365 pixels	RGB	3,651 images	2,921 images	730 images
Corn-Leaf-Diseases	256x256 pixels	RGB	3,000 images	2,500 images	500 images
Tomato-Leaf-Diseases	256x256 pixels	RGB	5,000 images	4,000 images	1,000 images
NASS	N/A	Statistical Data	Multi-year/multi-region table	N/A	N/A

Table 2

Summary of datasets used in the experiments below

**Figure 15:** Domain Adaptation Process for Four Experiments (Left) Source domain dataset. (Right) Target domain dataset.

5.1.1. Experimental Results

This section demonstrates the classification, detection, and prediction capabilities of deep domain adaptation in agricultural applications, using experimental results from plant disease detection, crop yield prediction, and remote sensing image agricultural land extraction. Since each algorithm uses a different experimental dataset, a common dataset is selected for comparison to more reasonably verify the anomaly detection performance of different algorithms on the same dataset. **Bold** and **red** text indicates the best performance of an algorithm on a specific dataset.

To evaluate the performance of plant disease detection models, we conducted four sets of experiments involving five datasets: PlantVillage [134], PlantDoc [135], Plant-Pathology [136], Corn-Leaf-Diseases, and Tomato-Leaf-Diseases. The PlantVillage dataset (PWD) was consistently used as the source domain in all experiments, as it was collected in a controlled laboratory environment, which provides a simpler background, thus facilitating model training and testing.

Table 3 presents the detailed results of MSUN across four experimental setups: C-PD, PVD-PP, PVD-CLD, and PVD-TLD. Compared to the multi-plant mixed transfer scenario in C-PD, single-plant transfer generally performs better. It is important to note that the symptoms of the same type of disease often appear similar on different plant leaves, which can lead to confusion in multi-plant transfer scenarios. However, in single-plant transfer tasks, the clearer intra-class boundaries help mitigate this issue. Additionally, the multi-representation modeling and subdomain alignment mechanisms introduced by MSUN effectively address the challenges of high inter-class similarity and large intra-class variance, enabling it to achieve excellent performance even in single-plant transfer.

In the plant disease transfer detection task, MSUN demonstrates significant advantages across various experimental configurations. Whether in multi-plant mixed transfer (C-PD) or single-plant transfer (PWD-PP, PVD-CLD, PVD-TLD), its average accuracy consistently outperforms existing mainstream methods. In the C-PD task, MSUN achieves an average accuracy of 56.06%, surpassing the baseline by more than 25 percentage points and clearly outperforming DSAN and MRAN, showcasing its strong adaptability under large domain shifts and complex class settings. In the PVD-PP experiment, MSUN achieves the highest accuracy across all three disease categories, with an average accuracy of 72.31%, significantly outperforming the second-best model, MRAN (67.45%), and the traditional method, DANN (50.04%). In PVD-CLD, MSUN achieves an impressive average accuracy of 96.78%, with particularly outstanding performance in the wilt disease category (93.81%) and the healthy category (84.77%), highlighting its powerful ability to extract key features and distinguish similar classes. The PVD-TLD task is more challenging, as it involves finer-grained disease categories and highly imbalanced class distributions, leading to poor performance from most methods. However, MSUN still achieves an average accuracy of 50.5%, especially excelling in the low-sample category "Septoria spot" with 80.79%, significantly outperforming other methods and demonstrating excellent intra-class generalization and cross-class discrimination capabilities. In summary, MSUN consistently maintains stable and leading performance across various transfer scenarios,

Task	Class / Crop	Baseline	DAAN	D-Coral	DAN	DANN	MRAN	DSAN	MSUN
C-PD	Apple	67.38	68.64	69.06	70.29	69.63	68.98	65.51	71.45
	Corn	50.07	48.81	49.11	52.15	48.11	49.87	51.39	56.46
	Grape	71.36	63.93	79.79	78.24	83.41	82.38	79.79	85.49
	Pepper bell	84.19	87.79	86.75	90.91	90.90	92.46	90.91	93.49
	Potato	50.34	63.66	66.06	64.72	62.33	57.82	64.19	67.42
	Tomato	30.17	39.82	43.32	46.23	49.51	49.34	45.75	48.67
PVD-PP	Average	30.78	33.08	33.37	33.79	39.71	39.84	42.87	56.06
	Gray spot	79.54	66.16	77.56	89.02	85.12	81.28	83.96	87.32
	Rust	24.10	55.81	33.42	34.99	30.26	52.57	35.42	57.71
	Healthy	11.02	36.64	48.05	11.84	28.71	70.87	51.24	73.86
PVD-CLD	Average	39.27	53.75	52.41	48.89	50.04	67.45	56.41	72.31
	Gray spot	61.49	78.57	79.44	68.29	76.66	79.22	81.71	80.09
	Blight	86.75	92.27	91.88	91.50	91.73	92.05	91.58	93.81
	Healthy	79.05	84.29	82.64	81.33	82.64	83.61	83.42	84.77
PVD-TLD	Rust	99.18	100.0	100.0	100.0	100.0	100.0	100.0	100.0
	Average	75.96	90.35	89.90	87.89	89.47	91.06	90.69	96.78
	Bacterial spot	5.34	10.23	12.50	12.22	8.24	18.47	10.51	29.27
	Healthy	70.61	83.75	85.81	83.41	86.92	75.92	92.03	78.67
PVD-TLD	Late blight	79.05	3.97	1.64	0.93	3.50	2.11	1.64	3.28
	Mold leaf	25.03	33.15	37.43	38.18	38.73	33.15	29.61	32.77
	Septoria spot	6.36	5.16	18.73	67.11	4.13	78.64	0.29	80.79
	Average	21.46	30.96	32.31	42.80	28.71	44.86	27.57	50.58

Table 3

Accuracy (%) results of the PVD-PD, PVD-PP, PVD-CLD, and PVD-TLD experiments.

fully validating the adaptability and effectiveness of its multi-representation and subdomain alignment mechanisms in agricultural image analysis. Compared to traditional domain adaptation methods, MSUN not only improves overall accuracy but also exhibits stronger robustness and generalization ability when dealing with complex tasks such as class imbalance, multi-disease coexistence, and cross-crop transfer. In the crop yield prediction experiments, the U.S. Corn Belt was chosen as the experimental region, being the world's largest corn-producing area with rich historical yield data. For model development and evaluation, three types of data were integrated: remote sensing products, meteorological observations, and yield records. The data primarily comes from the U.S. Department of Agriculture's National Agricultural Statistics Service (USDA NASS, 2020). The experiment includes both local experiments (training and testing in the same region) and cross-domain transfer experiments (training and testing in different regions). Multiple advanced machine learning models were compared, including traditional Random Forest (RF), Deep Neural Networks (DNN), the original adversarial domain adaptation model (DANN), and its improved version (ADANN).

The prediction results of each model under different years and experimental settings are shown in Table 4.

The results show that in local experiments, both DNN and RF perform consistently, with DNN particularly excelling in the ETF→ETF task. For example, in 2019, DNN achieved an R^2 of 0.71 in this task, marking the best performance of the year. This indicates that DNN has strong performance in same-domain data modeling, especially in scenarios with clear sample structure and abundant data.

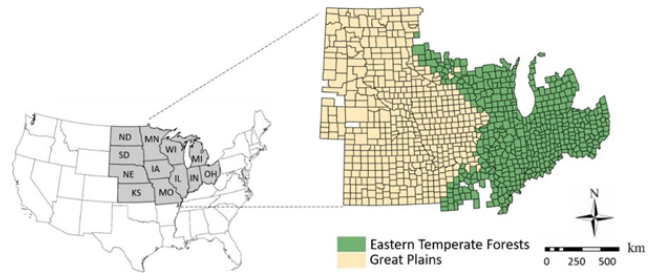


Figure 16: Corn planting counties in two ecosystem regions (i.e., ETF and GP) within the study area.

In contrast, in the cross-domain migration experiments (GP→ETF and ETF→GP), the performance of traditional models declined significantly. For instance, in 2019, RF's R^2 in ETF→GP was only 0.19, while in the local GP→GP task, it was 0.74. This reflects the model's poor generalization ability when dealing with domain differences. DNN faced similar issues, with migration prediction errors fluctuating and overall stability being poor.

Models incorporating adversarial mechanisms significantly outperformed traditional methods in cross-domain scenarios. Both DANN and ADANN outperformed RF and DNN, with ADANN being the most stable and superior. For example, in the 2019 ETF→GP experiment, ADANN achieved an R^2 of 0.73 and an RMSE of just 1.15, clearly outperforming DANN with 0.56 and 1.47, respectively. ADANN more effectively reduced the feature distribution

Year	Case	Metric	RF	DNN	DANN	ADANN
2016	GP→GP	R^2	0.75	0.81	0.64	0.85
		RMSE	1.39	1.18	1.65	1.05
	ETF→ETF	R^2	0.51	0.55	0.47	0.62
		RMSE	1.13	1.01	1.18	0.92
	GP→ETF	R^2	0.54	0.43	0.44	0.67
		RMSE	1.02	1.22	1.21	0.86
	ETF→GP	R^2	0.48	0.55	0.68	0.76
		RMSE	1.98	1.82	1.54	1.35
2017	GP→GP	R^2	0.73	0.75	0.74	0.77
		RMSE	1.34	1.26	1.30	1.24
	ETF→ETF	R^2	0.61	0.75	0.64	0.78
		RMSE	1.23	0.97	1.17	0.91
	GP→ETF	R^2	0.58	0.52	0.35	0.73
		RMSE	1.26	1.36	1.58	1.03
	ETF→GP	R^2	0.52	0.64	0.68	0.77
		RMSE	1.78	1.54	1.45	1.23
2018	GP→GP	R^2	0.76	0.79	0.81	0.84
		RMSE	1.11	1.05	1.00	0.91
	ETF→ETF	R^2	0.54	0.56	0.51	0.65
		RMSE	0.97	0.95	1.00	0.84
	GP→ETF	R^2	0.49	0.30	0.33	0.57
		RMSE	1.01	1.20	1.17	0.97
	ETF→GP	R^2	0.53	0.49	0.75	0.78
		RMSE	1.57	1.63	1.14	1.07
2019	GP→GP	R^2	0.74	0.73	0.53	0.76
		RMSE	1.14	1.15	1.53	1.08
	ETF→ETF	R^2	0.63	0.71	0.64	0.66
		RMSE	1.09	0.96	1.08	1.05
	GP→ETF	R^2	0.52	0.56	0.62	0.68
		RMSE	1.25	1.19	1.11	1.02
	ETF→GP	R^2	0.19	0.34	0.56	0.73
		RMSE	2.00	1.80	1.47	1.15

Table 4

Model comparison in different years.

differences between the source and target domains, improving cross-domain generalization through adversarial training and adaptive strategies.

Moreover, environmental changes in different years had a significant impact on model performance. In 2019, several regions experienced unusually wet weather, which weakened the correlation between remote sensing images and yield labels, exacerbating domain shift and further degrading the performance of traditional models. However, ADANN maintained high accuracy and stability under such extreme conditions, demonstrating strong robustness and adaptability.

Overall, the four-year experimental results show that ADANN consistently performs well in both local and cross-domain tasks, with particularly stronger accuracy and smaller errors in cross-domain predictions. In comparison, traditional models, while adequate in local predictions, struggle significantly with cross-domain tasks due to domain shift. With its stability, adaptability, and excellent generalization capabilities, ADANN emerges as the preferred solution for

cross-domain modeling in agricultural remote sensing yield prediction.

By analyzing the error space distribution (Figure 17), it was found that traditional models (RF, DNN) exhibited significant error clustering in regions far from the source domain, such as Michigan and Ohio. However, adversarial learning methods (DANN, ADANN) effectively mitigated these issues. ADANN further optimized the error distribution in key agricultural areas such as Illinois. From the overall error performance, ADANN, through adversarial learning, extracts more generalized domain-invariant features, effectively mitigating the distribution differences between the source and target domains and reducing prediction bias. Multi-year experiments conducted in the U.S. Corn Belt's two ecological regions show that ADANN outperforms RF, DNN, and the original DANN in both local and cross-domain experiments, maintaining superior prediction accuracy across all four testing years from 2016 to 2019. Its success lies in achieving a good balance between domain adversarial loss and prediction error, leading to more stable

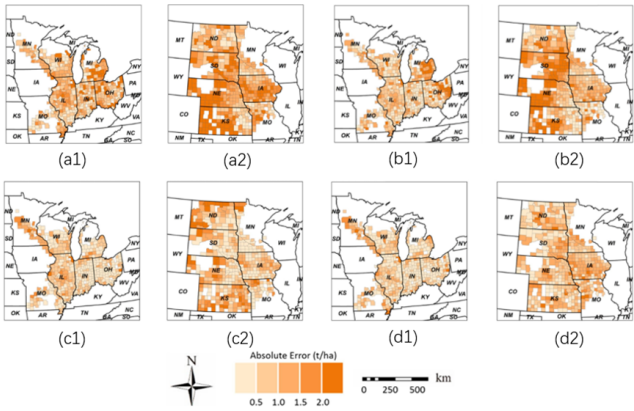


Figure 17: Mean absolute error maps from 2016 to 2019 for two migration experiments: (1) GP→ETF and (2) ETF→GP, for models (a) RF, (b) DNN, (c) DANN, and (d) ADANN.

and accurate yield predictions, demonstrating its practicality and advancement in cross-domain modeling for agricultural remote sensing.

In the comparative experiment for agricultural land extraction from remote sensing images, we selected six representative domain adaptation methods for performance evaluation, including the baseline method (source domain only, without domain adaptation), AdapSegNet [101], ADVENT [102], BDL [103], IntraDA [66], and TransFusion-DualDA [85]. The experiment used three agricultural land datasets with significant scale differences to test the model’s generalization capability: (1) The DeepGlobe dataset provides high-resolution farmland samples at 0.5 meters per pixel, with annotations that cover fine parcel boundary features; (2) The LoveDA dataset captures complex agricultural landscapes in urban-rural transition areas with ultra-high resolution at 0.3 meters per pixel; (3) The GID dataset, although lower in resolution (4 meters per pixel), effectively reflects regional-scale farmland distribution patterns due to its large coverage. Table 5 summarizes the quantitative evaluation results of five domain adaptation methods in cross-dataset testing, covering three resolution scenarios: DeepGlobe (0.5 m/pixel), LoveDA (0.3 m/pixel), and GID (4 m/pixel).

In all three dataset migration settings, TransFusion-DualDA consistently outperforms the other methods, particularly excelling in the core metrics IoU, COM, and F1, where it maintains the highest performance. In the DeepGlobe → LoveDA task, TransFusion-DualDA achieves an IoU of 55.763% and an F1 score of 67.750%, outperforming other methods (such as IntraDA and BDL) by 5-10 percentage points. This is primarily due to its Transformer backbone network’s strong global perception capability and multi-scale feature fusion structure at all levels, which allows it to effectively address cross-domain visual discrepancies.

In the GID → LoveDA migration task, TransFusion-DualDA shows a COM value of 92.109%, significantly outperforming other methods with a 32% improvement. This indicates its superior ability in spatial alignment of target

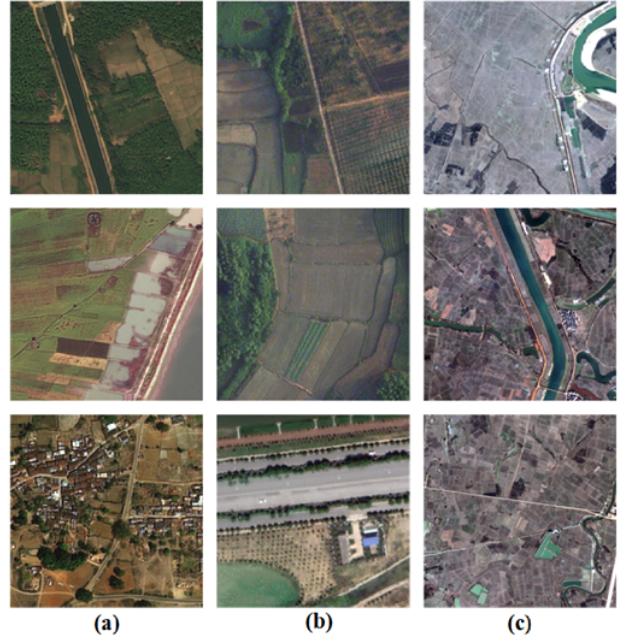


Figure 18: Sample images from three agricultural land datasets. (a) DeepGlobe dataset with a resolution of 0.5 m/pixel; (b) LoveDA dataset with a resolution of 0.3 m/pixel; (c) GID dataset with a resolution of 4 m/pixel.

boundary structures, particularly when adapting from the low-resolution source domain (GID, 4m/pixel) to the high-resolution target domain (LoveDA, 0.3m/pixel). The challenge of this task lies in the significant resolution gap and feature scale differences, which traditional methods struggle to handle. However, TransFusion-DualDA achieves better feature alignment through the Transformer’s long-distance dependency modeling capabilities. In the DeepGlobe (high resolution) to GID (low resolution) migration, TransFusion-DualDA still maintains the best performance (F1 = 62.439%, IoU = 49.553%), but the performance gap with IntraDA and BDL narrows. This could be because, at a resolution of 512×512 pixels, it becomes more challenging to extract stable and discriminative global features, and the lower information content of target domain images limits the effect of knowledge transfer from the source domain. This suggests that for high-to-low resolution cross-domain migration tasks, the model requires stronger feature redundancy handling and global modeling capabilities. Overall, TransFusion-DualDA excels in adapting to multi-resolution and cross-scenario domain differences, particularly leading in COM, F1, and IoU metrics. This validates the effectiveness of the Transformer backbone and full-level feature fusion in extracting domain-invariant representations. Its notable advantage in the COM metric underscores its strong ability to maintain target shape and boundaries, making it well-suited for tasks like remote sensing and agricultural plot classification that require structural preservation.

Source → Target	Method	IoU	COM	COR	F1
DeepGlobe → LoveDA	Source-only	36.327	45.895	62.861	49.108
	AdaptSegNet	46.921	74.478	55.190	60.404
	ADVENT	49.392	74.621	58.085	61.169
	BDL	52.234	79.747	59.011	65.334
	IntraDA	51.710	82.855	57.341	64.589
	TransFusion-DualDA	55.763	81.370	62.549	67.750
GID → LoveDA	Source-only	36.229	40.139	83.018	46.026
	AdaptSegNet	42.931	54.221	71.295	55.454
	ADVENT	45.035	60.762	65.021	58.250
	BDL	44.592	58.231	67.447	57.732
	IntraDA	48.254	60.365	72.898	60.799
	TransFusion-DualDA	53.470	92.109	56.891	66.042
DeepGlobe → GID	Source-only	26.986	39.204	62.884	36.599
	AdaptSegNet	43.098	68.614	59.414	56.067
	ADVENT	45.995	77.435	57.403	58.940
	BDL	46.348	75.789	58.373	59.508
	IntraDA	47.631	68.488	60.293	61.465
	TransFusion-DualDA	49.553	88.545	54.535	62.439

Table 5

DeepGlobe → LoveDA, GID → LoveDA, and DeepGlobe → GID experimental results comparison.

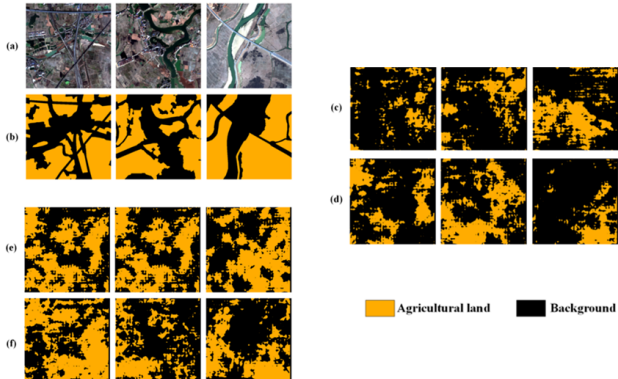
**Figure 19:** Visualization of segmentation results using different methods. (a) Target image; (b) Ground truth dataset; (c) Source-only; (d) ADVENT; (e) IntraDA; (f) TransFusion-DualDA.

Figure 19 shows the visualization results obtained under the DeepGlobe → GID UDA setting, using the methods Source-only, ADVENT, IntraDA, and TransFusion-DualDA. The results clearly demonstrate the necessity and effectiveness of unsupervised domain adaptation methods in cross-sensor remote sensing image segmentation. Without any domain adaptation method (c), the model performs poorly on the target domain, with agricultural land and background areas blending together. The predicted results show large areas of random noise and structural loss, indicating that the original model cannot handle the significant distribution shift caused by sensor differences. This proves that directly transferring the source domain model to the target domain leads to a sharp performance decline due to

inconsistent feature distributions. After applying ADVENT (d) and IntraDA (e), the segmentation performance improves significantly. ADVENT, by introducing adversarial training, reduces the domain feature shift, enhancing the recognition of agricultural areas. IntraDA further adds an intra-class consistency constraint, improving the connectivity and contour integrity of agricultural plots. However, both methods still suffer from issues like "boundary blurring" and "region fragmentation," indicating insufficient domain alignment and limited global structural understanding of the target domain. The results from TransFusion-DualDA (f) are the closest to the ground truth labels among the three methods. The predicted agricultural plots are not only highly consistent in overall contours but also show high accuracy in recognizing most detailed areas, reflecting its significant advantages in maintaining spatial structure and understanding global context. This is due to the long-range dependency modeling ability of the Transformer backbone network and the multi-scale feature fusion strategy, allowing the model to simultaneously focus on both local and global features. Nevertheless, some "fragmentation" and prediction noise at the boundaries are still observed, reflecting the challenges posed by heterogeneous feature distributions in high-resolution remote sensing images. In summary, the visual results validate the importance of unsupervised domain adaptation methods for cross-sensor agricultural land segmentation, with TransFusion-DualDA standing out through more in-depth feature alignment strategies to achieve more stable and precise target domain predictions, providing strong technical support for practical remote sensing agricultural monitoring.

5.2. Key Findings and Summary from the Experiments

In the plant disease transfer detection task, MSUN leads with an average accuracy of 56.06, outperforming other methods such as DSAN (42.87), particularly excelling in cross-domain classification of corn, grapes, sweet peppers, potatoes, and apples, demonstrating strong adaptability to complex agricultural scenarios. Although the detection accuracy for tomato diseases is slightly lower (48.67), DANN (49.51) and MRAN (49.34) could serve as potential optimization directions. For sweet pepper, with its distinctive morphological features, all methods achieved accuracy above 84%. The advantage of MSUN comes from its innovative design: multiple representation modules extract rich features to mitigate domain and class discrepancies, while sub-domain adaptation strengthens fine-grained semantic alignment, and uncertainty regularization effectively suppresses pseudo-label interference. These techniques make it excel in cross-species disease transfer and achieve optimal results on four public datasets, making it the preferred solution for improving multi-crop disease diagnosis generalization and accuracy. In the crop yield prediction experiment across different ecological regions of the U.S. Corn Belt, the comparison of RF, DNN, DANN, and ADANN models shows that ADANN consistently maintains the highest prediction accuracy in both local and cross-domain migration tasks from 2016 to 2019. For example, in the local experiment of 2019 (GP→GP), RF and DNN have R^2 values of 0.76 and 0.79, while ADANN improves to 0.85. In the cross-domain migration task (GP→ETF), RF and DNN drop to R^2 values of 0.49 and 0.30, while ADANN remains stable at 0.63, significantly outperforming DANN (0.58). Model analysis shows that ADANN effectively mitigates the impact of domain shift on prediction by balancing domain loss and prediction loss. Additionally, the error spatial distribution (Figure 3) reveals significant error clustering in areas like Michigan and Ohio for RF and DNN, while DANN partially alleviates these issues through adversarial training, and ADANN further optimizes error distribution in key areas such as Illinois, demonstrating its robustness in dynamic domain shift scenarios. In the comparison experiment for remote sensing agricultural land extraction, the TransFusion-DualDA method shows significant advantages, leading in core metrics such as IoU (55.763%) and F1 (67.750%) in the DeepGlobe → LoveDA cross-domain task, outperforming ADVENT and AdaptSegNet by 6-7%. In the migration from low-resolution GID (4m/pixel) to ultra-high-resolution LoveDA (0.3m/pixel), the IoU increases by 5.2%, and the F1 score rises by 6%, validating the effectiveness of its multi-scale feature fusion and Transformer backbone network in optimizing global-local feature cooperation. In the reverse task from high-resolution DeepGlobe (0.5m/pixel) to low-resolution GID, although the performance improvement is limited (F1 = 62.439%), it still outperforms methods like BDL. Visualization results (Figure 17) show that, compared to ADVENT and IntraDA, TransFusion-DualDA's segmentation boundaries are much closer to the ground truth, with

more complete coverage of agricultural land, although target domain noise remains, reflecting the challenge of local feature alignment within domains. The experimental results indicate that the method's domain-adversarial training and entropy-driven sub-domain partitioning strategy significantly mitigate cross-sensor data differences (e.g., complex landscapes in urban-rural transition areas), reducing reliance on manual labeling. Future work will need to further optimize the extraction of global features in high-resolution scenarios to enhance adaptability in dynamic remote sensing environments.

6. Challenges and Future Research Directions

Current research in agricultural intelligence faces multiple challenges, including data complexity, method adaptability, and technical limitations. This chapter identifies core issues from the perspective of field applications and suggests targeted research directions.

6.1. Model Adaptability Barriers in Field Scenarios

The unique characteristics of agricultural environments present three main obstacles for model application: Firstly, the challenge of multi-scale fusion of spatiotemporal data is prominently shown in the significant scale differences between satellite data (10-100m resolution), drone data (0.1-1m), and ground sensor data (centimeter-level). Existing 3D convolution methods struggle to achieve cross-scale feature alignment. Secondly, the issue of scarce labeled data is particularly severe in the field, where crop disease samples in typical agricultural scenarios often number fewer than 50 per class. Traditional transfer learning methods show a 30% accuracy drop when sample sizes are below 100. Thirdly, multimodal data collaboration faces physical constraints. For example, hyperspectral imaging is limited by fluctuations in field lighting ($\pm 30\%$ radiation intensity changes), leading to distribution shifts in cross-period data.

6.2. Key Future Research Directions

To address the above challenges, the following research directions are proposed: (1) Lightweight Spatiotemporal Modeling Framework Develop miniature network architectures with fewer than 1M parameters, integrating physical prior knowledge (e.g., crop growth models) to constrain feature learning. Focus on breakthroughs in spatiotemporal decoupling representation techniques to achieve feature-level fusion between drone images (5cm resolution) and satellite data (10m), reducing computational energy consumption to 1/5 of current 3D CNN methods. (2) Weakly Supervised Transfer Learning Paradigm Establish a pseudo-label generation mechanism for field scenes, leveraging temporal continuity (e.g., crop growth stages) to build cross-period self-supervised signals. Explore curriculum learning strategies based on field phenological patterns to maintain classification accuracy above 85% when the labeled sample size is less than 100. (3) Robust Multimodal Fusion System Design

illumination-invariant feature extraction modules to eliminate environmental interference through spectral normalization. Develop adversarial training methods based on physical information to maintain multimodal feature consistency under lighting fluctuations of $\pm 40\%$. Focus on resolving cross-view matching issues between drone and ground sensor data, establishing sub-meter spatial alignment standards. (4) Privacy-Preserving Collaborative Learning Optimize the communication efficiency of federated learning frameworks to achieve daily model updates under bandwidth constraints of less than 10Mbps. Develop differential privacy protection mechanisms to ensure parameter sharing complies with data regulations such as GDPR, maintaining a model performance loss of less than 5% at a privacy budget of $\epsilon = 2$. These research directions should be closely validated in real-world field operation scenarios. It is recommended to establish an open testing benchmark that includes more than 10 typical crops and covers at least three climate zones. Real-world constraints such as field noise (device errors $\pm 5\%$, occlusion rates of 20%) should also be incorporated to drive the transformation of research results into practical applications.

7. Conclusion

Adaptive models in agriculture face various challenges, especially when handling the complexity of spatiotemporal data, the scarcity of labeled data, and the heterogeneity of multimodal data. As agricultural environments become more complex, the adaptability of existing domain adaptation technologies in field environments still needs improvement, especially in cross-season and cross-region variations and dynamic agricultural scenarios. Future research can focus on key areas such as task-specific high-dimensional adaptive models, which will help improve model performance in different agricultural tasks (e.g., crop health monitoring, pest and disease recognition). Unsupervised domain adaptation is also a promising direction, as the scarcity of labeled data makes unsupervised learning-based models particularly valuable. Moreover, with the increasing diversity of agricultural data, researchers can explore multimodal data fusion as a breakthrough, combining image, meteorological, and soil information to further enhance model accuracy and generalization ability. Additionally, effective source-free domain adaptation remains one of the key future challenges when no source domain data is available.

The uniqueness of field environments requires more adjustments and optimizations to current technologies, especially when facing complex weather variations, lighting conditions, crop types, and differences in data collection methods. How to ensure that models can operate stably in such dynamic and complex field environments will be a critical factor influencing the widespread application of agricultural visual technologies. Addressing these challenges will help improve the precision, generalization, and cross-domain adaptability of agricultural image analysis, thereby advancing precision agriculture and intelligent agricultural

systems, and providing more efficient support for agricultural decision-making, crop prediction, and pest and disease monitoring.

References

- [1] A. Zhang, Y. Yang, J. Xu, X. Cao, X. Zhen, and L. Shao, "Latent domain generation for unsupervised domain adaptation object counting," *IEEE Transactions on Multimedia*, vol. 25, pp. 1773–1783, 2022.
- [2] J. Quiñonero-Candela, *Dataset shift in machine learning*. Mit Press, 2009.
- [3] R. N. Joglekar and N. Tiwari, "A review of deep learning techniques for identification and diagnosis of plant leaf disease," *Smart Trends in Computing and Communications: Proceedings of SmartCom 2020*, pp. 435–441, 2020.
- [4] Y. Jiang and C. Li, "Convolutional neural networks for image-based high-throughput plant phenotyping: a review," *Plant Phenomics*, 2020.
- [5] G. Csurka, "A comprehensive survey on domain adaptation for visual applications," *Domain adaptation in computer vision applications*, pp. 1–35, 2017.
- [6] M. Wang and W. Deng, "Deep visual domain adaptation: A survey," *Neurocomputing*, vol. 312, pp. 135–153, 2018.
- [7] G. Wilson and D. J. Cook, "A survey of unsupervised deep domain adaptation," *ACM Transactions on Intelligent Systems and Technology (TIST)*, vol. 11, no. 5, pp. 1–46, 2020.
- [8] W. M. Kouw and M. Loog, "A review of domain adaptation without target labels," *IEEE transactions on pattern analysis and machine intelligence*, vol. 43, no. 3, pp. 766–785, 2019.
- [9] V. M. Patel, R. Gopalan, R. Li, and R. Chellappa, "Visual domain adaptation: A survey of recent advances," *IEEE signal processing magazine*, vol. 32, no. 3, pp. 53–69, 2015.
- [10] S. Sun, H. Shi, and Y. Wu, "A survey of multi-source domain adaptation," *Information Fusion*, vol. 24, pp. 84–92, 2015.
- [11] S. Zhao, B. Li, P. Xu, and K. Keutzer, "Multi-source domain adaptation in the deep learning era: A systematic survey," *arXiv preprint arXiv:2002.12169*, 2020.
- [12] S. PanQ, "Yang, "a survey on transfer learning,"," *IEEE Trans. Knowl. Data Eng*, vol. 22, no. 10, pp. 1345–1359, 2010.
- [13] L. Shao, F. Zhu, and X. Li, "Transfer learning for visual categorization: A survey," *IEEE transactions on neural networks and learning systems*, vol. 26, no. 5, pp. 1019–1034, 2014.
- [14] J. Zhang, W. Li, P. Ogunbona, and D. Xu, "Recent advances in transfer learning for cross-dataset visual recognition: A problem-oriented perspective," *ACM Computing Surveys (CSUR)*, vol. 52, no. 1, pp. 1–38, 2019.
- [15] C. Tan, F. Sun, T. Kong, W. Zhang, C. Yang, and C. Liu, "A survey on deep transfer learning," in *Artificial Neural Networks and Machine Learning–ICANN 2018: 27th International Conference on Artificial Neural Networks, Rhodes, Greece, October 4–7, 2018, Proceedings, Part III 27*. Springer, 2018, pp. 270–279.
- [16] F. Zhuang, Z. Qi, K. Duan, D. Xi, Y. Zhu, H. Zhu, H. Xiong, and Q. He, "A comprehensive survey on transfer learning," *Proceedings of the IEEE*, vol. 109, no. 1, pp. 43–76, 2020.
- [17] R. Girshick, J. Donahue, T. Darrell, and J. Malik, "Rich feature hierarchies for accurate object detection and semantic segmentation," in *Proceedings of the IEEE conference on computer vision and pattern recognition*, 2014, pp. 580–587.
- [18] R. Girshick, "Fast r-cnn," in *Proceedings of the IEEE international conference on computer vision*, 2015, pp. 1440–1448.
- [19] R. Faster, "Towards real-time object detection with region proposal networks," *Advances in neural information processing systems*, vol. 9199, no. 10.5555, pp. 2969 239–2969 250, 2015.
- [20] A. Fuentes, S. Yoon, S. C. Kim, and D. S. Park, "A robust deep-learning-based detector for real-time tomato plant diseases and pests recognition," *Sensors*, vol. 17, no. 9, p. 2022, 2017.

- [21] M. Long, J. Wang, G. Ding, J. Sun, and P. S. Yu, "Transfer joint matching for unsupervised domain adaptation," in *Proceedings of the IEEE conference on computer vision and pattern recognition*, 2014, pp. 1410–1417.
- [22] M. A. Molina-Cabanillas, M. J. Jiménez-Navarro, R. Arjona, F. Martínez-Álvarez, and G. Asencio-Cortés, "Diafan-tl: An instance weighting-based transfer learning algorithm with application to phenology forecasting," *Knowledge-Based Systems*, vol. 254, p. 109644, 2022.
- [23] C. Yaras, K. Kassaw, B. Huang, K. Bradbury, and J. M. Malof, "Randomized histogram matching: A simple augmentation for unsupervised domain adaptation in overhead imagery," *IEEE Journal of Selected Topics in Applied Earth Observations and Remote Sensing*, vol. 17, pp. 1988–1998, 2023.
- [24] Y. Cui, L. Wang, J. Su, S. Gao, and L. Wang, "Iterative weighted active transfer learning hyperspectral image classification," *Journal of Applied Remote Sensing*, vol. 15, no. 3, pp. 032 207–032 207, 2021.
- [25] H. Li, J. Li, Y. Zhao, M. Gong, Y. Zhang, and T. Liu, "Cost-sensitive self-paced learning with adaptive regularization for classification of image time series," *IEEE Journal of Selected Topics in Applied Earth Observations and Remote Sensing*, vol. 14, pp. 11 713–11 727, 2021.
- [26] D. Tuia, C. Persello, and L. Bruzzone, "Domain adaptation for the classification of remote sensing data: An overview of recent advances," *IEEE geoscience and remote sensing magazine*, vol. 4, no. 2, pp. 41–57, 2016.
- [27] M. Wang, D. Zhang, J. Huang, P.-T. Yap, D. Shen, and M. Liu, "Identifying autism spectrum disorder with multi-site fmri via low-rank domain adaptation," *IEEE Transactions on Medical Imaging*, vol. 39, no. 3, pp. 644–655, 2020.
- [28] B. Fernando, A. Habrard, M. Sebban, and T. Tuytelaars, "Unsupervised visual domain adaptation using subspace alignment," in *Proceedings of the IEEE international conference on computer vision*, 2013, pp. 2960–2967.
- [29] B. Sun, J. Feng, and K. Saenko, "Return of frustratingly easy domain adaptation," in *Proceedings of the Thirtieth AAAI Conference on Artificial Intelligence*, ser. AAAI'16. AAAI Press, 2016, p. 2058–2065.
- [30] J. Peng, W. Sun, T. Wei, and W. Fan, "A modified correlation alignment algorithm for the domain adaptation of gf-5 hyperspectral image," *Journal of Remote Sensing (Chinese)*, vol. 24, no. 4, pp. 417–426, 2020.
- [31] F. Weilandt, R. Behling, R. Goncalves, A. Madadi, L. Richter, T. Sanona, D. Spengler, and J. Welsch, "Early crop classification via multi-modal satellite data fusion and temporal attention," *Remote Sensing*, vol. 15, no. 3, p. 799, 2023.
- [32] J. Li, Y. Shen, and C. Yang, "An adversarial generative network for crop classification from remote sensing timeseries images," *Remote Sensing*, vol. 13, no. 1, p. 65, 2020.
- [33] Y. Wang, H. Huang, and R. State, "Cross domain early crop mapping with label spaces discrepancies using multicropgan," *ISPRS Annals of the Photogrammetry, Remote Sensing and Spatial Information Sciences*, vol. 10, pp. 241–248, 2024.
- [34] K. Takahashi, H. Madokoro, S. Yamamoto, Y. Nishimura, S. Nix, H. Woo, T. K. Saito, and K. Sato, "Domain adaptation for agricultural image recognition and segmentation using category maps," in *2021 21st International Conference on Control, Automation and Systems (ICCAS)*. IEEE, 2021, pp. 1680–1685.
- [35] L. Bruzzone and C. Persello, "A novel approach to the selection of spatially invariant features for the classification of hyperspectral images with improved generalization capability," *IEEE transactions on geoscience and remote sensing*, vol. 47, no. 9, pp. 3180–3191, 2009.
- [36] C. Persello and L. Bruzzone, "Kernel-based domain-invariant feature selection in hyperspectral images for transfer learning," *IEEE transactions on geoscience and remote sensing*, vol. 54, no. 5, pp. 2615–2626, 2015.
- [37] C. Paris and L. Bruzzone, "A sensor-driven hierarchical method for domain adaptation in classification of remote sensing images," *IEEE Transactions on Geoscience and Remote Sensing*, vol. 56, no. 3, pp. 1308–1324, 2017.
- [38] L. Yan, R. Zhu, Y. Liu, and N. Mo, "Tradaboost based on improved particle swarm optimization for cross-domain scene classification with limited samples," *IEEE Journal of Selected Topics in Applied Earth Observations and Remote Sensing*, vol. 11, no. 9, pp. 3235–3251, 2018.
- [39] Y. Tang and X. Li, "Set-based similarity learning in subspace for agricultural remote sensing classification," *Neurocomputing*, vol. 173, pp. 332–338, 2016.
- [40] B. Banerjee and S. Chaudhuri, "Hierarchical subspace learning based unsupervised domain adaptation for cross-domain classification of remote sensing images," *IEEE Journal of Selected Topics in Applied Earth Observations and Remote Sensing*, vol. 10, no. 11, pp. 5099–5109, 2017.
- [41] E. Aptoula and B. Yanikoglu, "Morphological features for leaf based plant recognition," in *2013 IEEE International Conference on Image Processing*. IEEE, 2013, pp. 1496–1499.
- [42] S. J. Pan, I. W. Tsang, J. T. Kwok, and Q. Yang, "Domain adaptation via transfer component analysis," *IEEE transactions on neural networks*, vol. 22, no. 2, pp. 199–210, 2010.
- [43] L. Bruzzone and D. F. Prieto, "Unsupervised retraining of a maximum likelihood classifier for the analysis of multitemporal remote sensing images," *IEEE Transactions on Geoscience and Remote Sensing*, vol. 39, no. 2, pp. 456–460, 2002.
- [44] —, "A partially unsupervised cascade classifier for the analysis of multitemporal remote-sensing images," *Pattern Recognition Letters*, vol. 23, no. 9, pp. 1063–1071, 2002.
- [45] L. Bruzzone and R. Cossu, "A multiple-cascade-classifier system for a robust and partially unsupervised updating of land-cover maps," *IEEE Transactions on Geoscience and Remote Sensing*, vol. 40, no. 9, pp. 1984–1996, 2002.
- [46] L. Bruzzone, R. Cossu, and G. Vernazza, "Combining parametric and non-parametric algorithms for a partially unsupervised classification of multitemporal remote-sensing images," *Information Fusion*, vol. 3, no. 4, pp. 289–297, 2002.
- [47] S. Zhong and Y. Zhang, "An iterative training sample updating approach for domain adaptation in hyperspectral image classification," *IEEE Geoscience and Remote Sensing Letters*, vol. 18, no. 10, pp. 1821–1825, 2020.
- [48] H. Wei, L. Ma, Y. Liu, and Q. Du, "Combining multiple classifiers for domain adaptation of remote sensing image classification," *IEEE Journal of Selected Topics in Applied Earth Observations and Remote Sensing*, vol. 14, pp. 1832–1847, 2021.
- [49] J. Zhang, J. Liu, B. Pan, Z. Chen, X. Xu, and Z. Shi, "An open set domain adaptation algorithm via exploring transferability and discriminability for remote sensing image scene classification," *IEEE Transactions on Geoscience and Remote Sensing*, vol. 60, pp. 1–12, 2021.
- [50] S. Xu, X. Mu, D. Chai, and S. Wang, "Adapting remote sensing to new domain with elm parameter transfer," *IEEE Geoscience and Remote Sensing Letters*, vol. 14, no. 9, pp. 1618–1622, 2017.
- [51] S. Rajan, J. Ghosh, and M. M. Crawford, "Exploiting class hierarchies for knowledge transfer in hyperspectral data," *IEEE Transactions on Geoscience and Remote Sensing*, vol. 44, no. 11, pp. 3408–3417, 2006.
- [52] L. Bruzzone and M. Marconcini, "Domain adaptation problems: A dasvm classification technique and a circular validation strategy," *IEEE transactions on pattern analysis and machine intelligence*, vol. 32, no. 5, pp. 770–787, 2009.
- [53] C. Deng, X. Liu, C. Li, and D. Tao, "Active multi-kernel domain adaptation for hyperspectral image classification," *Pattern Recognition*, vol. 77, pp. 306–315, 2018.
- [54] I. Kalita, R. N. S. Kumar, and M. Roy, "Deep learning-based cross-sensor domain adaptation under active learning for land cover classification," *IEEE Geoscience and Remote Sensing Letters*, vol. 19,

- pp. 1–5, 2021.
- [55] A. Saboori, H. Ghassemian, and F. Razzazi, “Active multiple kernel fredholm learning for hyperspectral images classification,” *IEEE Geoscience and Remote Sensing Letters*, vol. 18, no. 2, pp. 356–360, 2020.
- [56] E. Izquierdo-Verdiguier, V. Laparra, L. Gomez-Chova, and G. Camps-Valls, “Encoding invariances in remote sensing image classification with svm,” *IEEE Geoscience and Remote Sensing Letters*, vol. 10, no. 5, pp. 981–985, 2012.
- [57] J. Wang, Y. Chen, H. Yu, M. Huang, and Q. Yang, “Easy transfer learning by exploiting intra-domain structures,” in *2019 IEEE international conference on multimedia and expo (ICME)*. IEEE, 2019, pp. 1210–1215.
- [58] Y. Zhu, F. Zhuang, J. Wang, J. Chen, Z. Shi, W. Wu, and Q. He, “Multi-representation adaptation network for cross-domain image classification,” *Neural Networks*, vol. 119, pp. 214–221, 2019.
- [59] B. Espejo-Garcia, N. Mylonas, L. Athanasakos, E. Vali, and S. Fountas, “Combining generative adversarial networks and agricultural transfer learning for weeds identification,” vol. 204. Elsevier, 2021, pp. 79–89.
- [60] R. Lu, N. Wang, Y. Zhang, Y. Lin, W. Wu, and Z. Shi, “Extraction of agricultural fields via dasfnet with dual attention mechanism and multi-scale feature fusion in south xinjiang, china,” *Remote Sensing*, vol. 14, no. 9, p. 2253, 2022.
- [61] Z. Li, S. Chen, X. Meng, R. Zhu, J. Lu, L. Cao, and P. Lu, “Full convolution neural network combined with contextual feature representation for cropland extraction from high-resolution remote sensing images,” *Remote Sensing*, vol. 14, no. 9, p. 2157, 2022.
- [62] R. Shang, J. Zhang, L. Jiao, Y. Li, N. Marturi, and R. Stolkin, “Multi-scale adaptive feature fusion network for semantic segmentation in remote sensing images,” *Remote Sensing*, vol. 12, no. 5, p. 872, 2020.
- [63] X. Zhang, B. Cheng, J. Chen, and C. Liang, “High-resolution boundary refined convolutional neural network for automatic agricultural greenhouses extraction from gaofen-2 satellite imageries,” *Remote Sensing*, vol. 13, no. 21, p. 4237, 2021.
- [64] M. Cordts, M. Omran, S. Ramos, T. Rehfeld, M. Enzweiler, R. Benenson, U. Franke, S. Roth, and B. Schiele, “The cityscapes dataset for semantic urban scene understanding,” in *Proceedings of the IEEE conference on computer vision and pattern recognition*, 2016, pp. 3213–3223.
- [65] A. Ghanbari, G. H. Shirdel, and F. Maleki, “Semi-self-supervised domain adaptation: Developing deep learning models with limited annotated data for wheat head segmentation,” *Algorithms*, vol. 17, no. 6, p. 267, 2024.
- [66] F. Pan, I. Shin, F. Rameau, S. Lee, and I. S. Kweon, “Unsupervised intra-domain adaptation for semantic segmentation through self-supervision,” in *2020 IEEE/CVF Conference on Computer Vision and Pattern Recognition (CVPR)*, 2020, pp. 3763–3772.
- [67] V. Rani, S. T. Nabi, M. Kumar, A. Mittal, and K. Kumar, “Self-supervised learning: A succinct review,” *Archives of Computational Methods in Engineering*, vol. 30, no. 4, pp. 2761–2775, 2023.
- [68] K. Najafian, L. Jin, H. R. Kutcher, M. Hladun, S. Horovatin, M. A. Oviedo-Ludena, S. M. P. De Andrade, L. Wang, and I. Stavness, “Detection of fusarium damaged kernels in wheat using deep semi-supervised learning on a novel wheatseedbelt dataset,” in *Proceedings of the IEEE/CVF International Conference on Computer Vision*, 2023, pp. 660–669.
- [69] K. Najafian, A. Ghanbari, I. Stavness, L. Jin, G. H. Shirdel, and F. Maleki, “A semi-self-supervised learning approach for wheat head detection using extremely small number of labeled samples,” in *Proceedings of the IEEE/CVF International Conference on Computer Vision*, 2021, pp. 1342–1351.
- [70] K. Najafian, A. Ghanbari, M. Sabet Kish, M. Eramian, G. H. Shirdel, I. Stavness, L. Jin, and F. Maleki, “Semi-self-supervised learning for semantic segmentation in images with dense patterns,” *Plant Phenomics*, vol. 5, p. 0025, 2023.
- [71] L. Yang, H. Wenhui, Y. Huihuang, R. Yuan, W. Tan, J. Xiu, and Z. Jun, “Tomato detection method using domain adaptive learning for dense planting environments.” vol. 40, no. 13, 2024.
- [72] Y. Zhu, F. Zhuang, J. Wang, G. Ke, J. Chen, J. Bian, H. Xiong, and Q. He, “Deep subdomain adaptation network for image classification,” *IEEE transactions on neural networks and learning systems*, vol. 32, no. 4, pp. 1713–1722, 2020.
- [73] W. Teng, N. Wang, H. Shi, Y. Liu, and J. Wang, “Classifier-constrained deep adversarial domain adaptation for cross-domain semisupervised classification in remote sensing images,” *IEEE Geoscience and Remote Sensing Letters*, vol. 17, no. 5, pp. 789–793, 2019.
- [74] X. Liu, X. Liu, B. Hu, W. Ji, F. Xing, J. Lu, J. You, C.-C. J. Kuo, G. El Fakhri, and J. Woo, “Suosis,” in *Proceedings of the AAAI conference on artificial intelligence*, vol. 35, no. 3, 2021, pp. 2189–2197.
- [75] X. Liu, F. Xing, J. You, J. Lu, C.-C. J. Kuo, G. El Fakhri, and J. Woo, “Subtype-aware dynamic unsupervised domain adaptation,” *IEEE Transactions on Neural Networks and Learning Systems*, vol. 35, no. 2, pp. 2820–2834, 2022.
- [76] X. Yang, L. Jiao, and Q. Pan, “Transfer adaptation learning for target recognition in sar images: A survey,” *IEEE Journal of Selected Topics in Applied Earth Observations and Remote Sensing*, 2024.
- [77] I. J. Goodfellow, J. Pouget-Abadie, M. Mirza, B. Xu, D. Warde-Farley, S. Ozair, A. Courville, and Y. Bengio, “Generative adversarial nets,” *Advances in neural information processing systems*, vol. 27, 2014.
- [78] Y. Ganin and V. Lempitsky, “Unsupervised domain adaptation by backpropagation,” in *International conference on machine learning*. PMLR, 2015, pp. 1180–1189.
- [79] Y. LeCun, “The mnist database of handwritten digits,” <http://yann.lecun.com/exdb/mnist/>, 1998.
- [80] F. Yu, A. Seff, Y. Zhang, S. Song, T. Funkhouser, and J. Xiao, “Lsun: Construction of a large-scale image dataset using deep learning with humans in the loop,” *arXiv preprint arXiv:1506.03365*, 2015.
- [81] A. Krizhevsky, G. Hinton *et al.*, “Learning multiple layers of features from tiny images,” 2009.
- [82] O. Russakovsky, J. Deng, H. Su, J. Krause, S. Satheesh, S. Ma, Z. Huang, A. Karpathy, A. Khosla, M. Bernstein *et al.*, “Imagenet large scale visual recognition challenge,” *International journal of computer vision*, vol. 115, pp. 211–252, 2015.
- [83] P. Shamsolmoali, M. Zareapoor, H. Zhou, R. Wang, and J. Yang, “Road segmentation for remote sensing images using adversarial spatial pyramid networks,” *IEEE Transactions on Geoscience and Remote Sensing*, vol. 59, no. 6, pp. 4673–4688, 2020.
- [84] G.-H. Kwak and N.-W. Park, “Unsupervised domain adaptation with adversarial self-training for crop classification using remote sensing images,” *Remote Sensing*, vol. 14, no. 18, p. 4639, 2022.
- [85] J. Zhang, S. Xu, J. Sun, D. Ou, X. Wu, and M. Wang, “Unsupervised adversarial domain adaptation for agricultural land extraction of remote sensing images,” *Remote Sensing*, vol. 14, no. 24, p. 6298, 2022.
- [86] S. Ji, D. Wang, and M. Luo, “Generative adversarial network-based full-space domain adaptation for land cover classification from multiple-source remote sensing images,” *IEEE Transactions on Geoscience and Remote Sensing*, vol. 59, no. 5, pp. 3816–3828, 2020.
- [87] O. Tasar, Y. Tarabalka, A. Giros, P. Alliez, and S. Clerc, “Standardgan: Multi-source domain adaptation for semantic segmentation of very high resolution satellite images by data standardization,” in *Proceedings of the IEEE/CVF Conference on Computer Vision and Pattern Recognition Workshops*, 2020, pp. 192–193.
- [88] D. Wittich and F. Rottensteiner, “Appearance based deep domain adaptation for the classification of aerial images,” *ISPRS Journal of Photogrammetry and Remote Sensing*, vol. 180, pp. 82–102, 2021.
- [89] W. Liu and F. Su, “A novel unsupervised adversarial domain adaptation network for remotely sensed scene classification,” *International Journal of Remote Sensing*, vol. 41, no. 16, pp. 6099–6116, 2020.
- [90] L. Yan, B. Fan, H. Liu, C. Huo, S. Xiang, and C. Pan, “Triplet adversarial domain adaptation for pixel-level classification of vhr

- remote sensing images,” *IEEE Transactions on Geoscience and Remote Sensing*, vol. 58, no. 5, pp. 3558–3573, 2019.
- [91] Y. Huang, J. Peng, N. Chen, W. Sun, Q. Du, K. Ren, and K. Huang, “Cross-scene wetland mapping on hyperspectral remote sensing images using adversarial domain adaptation network,” *ISPRS Journal of Photogrammetry and Remote Sensing*, vol. 203, pp. 37–54, 2023.
- [92] M. B. Bejiga, F. Melgani, and P. Beraldini, “Domain adversarial neural networks for large-scale land cover classification,” *Remote Sensing*, vol. 11, no. 10, p. 1153, 2019.
- [93] M. M. Al Rahhal, Y. Bazi, H. Al-Hwiti, H. Alhichri, and N. Alajlan, “Adversarial learning for knowledge adaptation from multiple remote sensing sources,” *IEEE Geoscience and Remote Sensing Letters*, vol. 18, no. 8, pp. 1451–1455, 2020.
- [94] A. Elshamli, G. W. Taylor, A. Berg, and S. Areibi, “Domain adaptation using representation learning for the classification of remote sensing images,” *IEEE Journal of Selected Topics in Applied Earth Observations and Remote Sensing*, vol. 10, no. 9, pp. 4198–4209, 2017.
- [95] M. Martini, V. Mazzia, A. Khalil, and M. Chiaberge, “Domain-adversarial training of self-attention-based networks for land cover classification using multi-temporal sentinel-2 satellite imagery,” *Remote Sensing*, vol. 13, no. 13, p. 2564, 2021.
- [96] G. Mateo-García, V. Laparra, D. López-Puigdolers, and L. Gómez-Chova, “Cross-sensor adversarial domain adaptation of landsat-8 and proba-v images for cloud detection,” *IEEE Journal of Selected Topics in Applied Earth Observations and Remote Sensing*, vol. 14, pp. 747–761, 2020.
- [97] L. Ma and J. Song, “Deep neural network-based domain adaptation for classification of remote sensing images,” *Journal of Applied Remote Sensing*, vol. 11, no. 4, pp. 042612–042612, 2017.
- [98] L. Zhang, M. Lan, J. Zhang, and D. Tao, “Stagewise unsupervised domain adaptation with adversarial self-training for road segmentation of remote-sensing images,” *IEEE Transactions on Geoscience and Remote Sensing*, vol. 60, pp. 1–13, 2021.
- [99] J. Guo, J. Yang, H. Yue, X. Liu, and K. Li, “Unsupervised domain-invariant feature learning for cloud detection of remote sensing images,” *IEEE Transactions on Geoscience and Remote Sensing*, vol. 60, pp. 1–15, 2021.
- [100] J. Hoffman, D. Wang, F. Yu, and T. Darrell, “Fcns in the wild: Pixel-level adversarial and constraint-based adaptation,” *arXiv preprint arXiv:1612.02649*, 2016.
- [101] Y.-H. Tsai, W.-C. Hung, S. Schulter, K. Sohn, M.-H. Yang, and M. Chandraker, “Learning to adapt structured output space for semantic segmentation,” in *Proceedings of the IEEE conference on computer vision and pattern recognition*, 2018, pp. 7472–7481.
- [102] T.-H. Vu, H. Jain, M. Bucher, M. Cord, and P. Pérez, “Advent: Adversarial entropy minimization for domain adaptation in semantic segmentation,” in *Proceedings of the IEEE/CVF conference on computer vision and pattern recognition*, 2019, pp. 2517–2526.
- [103] Y. Li, L. Yuan, and N. Vasconcelos, “Bidirectional learning for domain adaptation of semantic segmentation,” in *Proceedings of the IEEE/CVF conference on computer vision and pattern recognition*, 2019, pp. 6936–6945.
- [104] X. Zhang, X. Yao, X. Feng, G. Cheng, and J. Han, “Dfnet for domain adaptation-based remote sensing scene classification,” *IEEE Transactions on Geoscience and Remote Sensing*, vol. 60, pp. 1–11, 2021.
- [105] J. Zheng, W. Wu, S. Yuan, Y. Zhao, W. Li, L. Zhang, R. Dong, and H. Fu, “A two-stage adaptation network (tsan) for remote sensing scene classification in single-source-mixed-multiple-target domain adaptation (s^2m^2t da) scenarios,” *IEEE Transactions on Geoscience and Remote Sensing*, vol. 60, pp. 1–13, 2021.
- [106] N. Makkar, L. Yang, and S. Prasad, “Adversarial learning based discriminative domain adaptation for geospatial image analysis,” *IEEE Journal of Selected Topics in Applied Earth Observations and Remote Sensing*, vol. 15, pp. 150–162, 2021.
- [107] K. Saito, S. Yamamoto, Y. Ushiku, and T. Harada, “Open set domain adaptation by backpropagation,” in *Proceedings of the European conference on computer vision (ECCV)*, 2018, pp. 153–168.
- [108] A. Farahani, S. Voghoei, K. Rasheed, and H. R. Arabnia, “A brief review of domain adaptation,” *Advances in data science and information engineering: proceedings from IC DATA 2020 and IKE 2020*, pp. 877–894, 2021.
- [109] M. Long, Y. Cao, J. Wang, and M. Jordan, “Learning transferable features with deep adaptation networks,” in *International conference on machine learning*. PMLR, 2015, pp. 97–105.
- [110] M. Baktashmotlagh, M. T. Harandi, B. C. Lovell, and M. Salzmann, “Unsupervised domain adaptation by domain invariant projection,” in *Proceedings of the IEEE international conference on computer vision*, 2013, pp. 769–776.
- [111] J. Shen, Y. Qu, W. Zhang, and Y. Yu, “Wasserstein distance guided representation learning for domain adaptation,” in *Proceedings of the AAAI conference on artificial intelligence*, vol. 32, no. 1, 2018.
- [112] B. Sun and K. Saenko, “Deep coral: Correlation alignment for deep domain adaptation,” in *Computer vision–ECCV 2016 workshops: Amsterdam, the Netherlands, October 8–10 and 15–16, 2016, proceedings, part III 14*. Springer, 2016, pp. 443–450.
- [113] A. dos Santos Ferreira, J. M. Junior, H. Pistori, F. Melgani, and W. N. Gonçalves, “Unsupervised domain adaptation using transformers for sugarcane rows and gaps detection,” *Computers and Electronics in Agriculture*, vol. 203, p. 107480, 2022.
- [114] M. Long, H. Zhu, J. Wang, and M. I. Jordan, “Deep transfer learning with joint adaptation networks,” in *International conference on machine learning*. PMLR, 2017, pp. 2208–2217.
- [115] Y. Zhu, F. Zhuang, J. Wang, J. Chen, Z. Shi, W. Wu, and Q. He, “Multi-representation adaptation network for cross-domain image classification,” *Neural Networks*, vol. 119, pp. 214–221, 2019.
- [116] Y. Zhu, F. Zhuang, J. Wang, G. Ke, J. Chen, J. Bian, H. Xiong, and Q. He, “Deep subdomain adaptation network for image classification,” *IEEE transactions on neural networks and learning systems*, vol. 32, no. 4, pp. 1713–1722, 2020.
- [117] S. Zhao, X. Yue, S. Zhang, B. Li, H. Zhao, B. Wu, R. Krishna, J. E. Gonzalez, A. L. Sangiovanni-Vincentelli, S. A. Seshia *et al.*, “A review of single-source deep unsupervised visual domain adaptation,” *IEEE Transactions on Neural Networks and Learning Systems*, vol. 33, no. 2, pp. 473–493, 2020.
- [118] Q. Zhu, Y. Sun, Q. Guan, L. Wang, and W. Lin, “A weakly pseudo-supervised decorrelated subdomain adaptation framework for cross-domain land-use classification,” *IEEE Transactions on Geoscience and Remote Sensing*, vol. 60, pp. 1–13, 2022.
- [119] Y. Li, Z. Cao, H. Lu, and W. Xu, “Unsupervised domain adaptation for in-field cotton boll status identification,” *Computers and Electronics in Agriculture*, vol. 178, p. 105745, 2020.
- [120] A. S. Garea, D. B. Heras, and F. Argüello, “Tcanet for domain adaptation of hyperspectral images,” *Remote Sensing*, vol. 11, no. 19, p. 2289, 2019.
- [121] Z. Li, X. Tang, W. Li, C. Wang, C. Liu, and J. He, “A two-stage deep domain adaptation method for hyperspectral image classification,” *Remote Sensing*, vol. 12, no. 7, p. 1054, 2020.
- [122] Y. Zhang, W. Li, M. Zhang, Y. Qu, R. Tao, and H. Qi, “Topological structure and semantic information transfer network for cross-scene hyperspectral image classification,” *IEEE Transactions on Neural Networks and Learning Systems*, 2021.
- [123] W. Wang, L. Ma, M. Chen, and Q. Du, “Joint correlation alignment-based graph neural network for domain adaptation of multitemporal hyperspectral remote sensing images,” pp. 3170–3184, 2021.
- [124] X. Liang, Y. Zhang, and J. Zhang, “Attention multisource fusion-based deep few-shot learning for hyperspectral image classification,” *IEEE Journal of Selected Topics in Applied Earth Observations and Remote Sensing*, vol. 14, pp. 8773–8788, 2021.
- [125] K. Yan, X. Guo, Z. Ji, and X. Zhou, “Deep transfer learning for cross-species plant disease diagnosis adapting mixed subdomains,” *IEEE/ACM transactions on computational biology and bioinformatics*, vol. 20, no. 4, pp. 2555–2564, 2021.
- [126] A. Fuentes, S. Yoon, T. Kim, and D. S. Park, “Open set self and across domain adaptation for tomato disease recognition with deep

- learning techniques,” *Frontiers in plant science*, vol. 12, p. 758027, 2021.
- [127] X. Wu, X. Fan, P. Luo, S. D. Choudhury, T. Tjahjadi, and C. Hu, “From laboratory to field: Unsupervised domain adaptation for plant disease recognition in the wild,” *Plant Phenomics*, vol. 5, p. 0038, 2023.
- [128] E. Othman, Y. Bazi, F. Melgani, H. Alhichri, N. Alajlan, and M. Zuair, “Domain adaptation network for cross-scene classification,” *IEEE Transactions on Geoscience and Remote Sensing*, vol. 55, no. 8, pp. 4441–4456, 2017.
- [129] X. Lu, T. Gong, and X. Zheng, “Multisource compensation network for remote sensing cross-domain scene classification,” *IEEE Transactions on Geoscience and Remote Sensing*, vol. 58, no. 4, pp. 2504–2515, 2019.
- [130] S. Zhu, B. Du, L. Zhang, and X. Li, “Attention-based multiscale residual adaptation network for cross-scene classification,” *IEEE Transactions on Geoscience and Remote Sensing*, vol. 60, pp. 1–15, 2021.
- [131] J. Geng, X. Deng, X. Ma, and W. Jiang, “Transfer learning for sar image classification via deep joint distribution adaptation networks,” *IEEE Transactions on Geoscience and Remote Sensing*, vol. 58, no. 8, pp. 5377–5392, 2020.
- [132] T. J. Young, T. Z. Jubery, C. N. Carley, M. Carroll, S. Sarkar, A. K. Singh, A. Singh, and B. Ganapathysubramanian, ““canopy fingerprints” for characterizing three-dimensional point cloud data of soybean canopies,” *Frontiers in plant science*, vol. 14, p. 1141153, 2023.
- [133] R. Zhao, Y. Zhu, and Y. Li, “Cla: A self-supervised contrastive learning method for leaf disease identification with domain adaptation,” *Computers and Electronics in Agriculture*, vol. 211, p. 107967, 2023.
- [134] S. P. Mohanty, D. P. Hughes, and M. Salathé, “Using deep learning for image-based plant disease detection,” *Frontiers in plant science*, vol. 7, p. 215232, 2016.
- [135] D. Singh, N. Jain, P. Jain, P. Kayal, S. Kumawat, and N. Batra, “Plant-doc: A dataset for visual plant disease detection,” in *Proceedings of the 7th ACM IKDD CoDS and 25th COMAD*, 2020, pp. 249–253.
- [136] R. Thapa, K. Zhang, N. Snavely, S. Belongie, and A. Khan, “The plant pathology challenge 2020 data set to classify foliar disease of apples,” *Applications in plant sciences*, vol. 8, no. 9, p. e11390, 2020.